NASA CR-112052

DESIGN, FABRICATION AND TESTING OF
TWO ELECTROHYDRAULIC VIBRATION ISOLATION SYSTEMS
FOR HELICOPTER ENVIRONMENTS

By Rush E. Allen and Peter C. Calcaterra

Distribution of this report is provided in the interest of
information exchange. Responsibility for the contents
resides in the author or organization that prepared it.

NATIONAL AERONAUTICS AND SPACE ADMINISTRATION

CONTENTS

Page

DESIGN, FABRICATION AND TESTING OF

TWO ELECTROHYDRAULIC VIBRATION ISOLATION SYSTEMS

FOR HELICOPTER ENVIRONMENTS

By Rush E. Allen and Peter C. Calcaterra

SUMMARY

Two electrohydraulic vibration isolation systems were designed and fabricated to reduce the vertical vibrations transmitted to the XH-51N research helicopter cabin at the blade passage frequency (18 Hz) and its first harmonic (36 Hz). Hydraulic power and electrical control are provided to two separate servoactuators from a common power supply and control electronics package located behind the pilot's seat. One servoactuator is installed between the cabin and fuselage and replaces an existing passive spring. A second servo-actuator is mounted between the existing seat and cabin floor. Both servo-actuators incorporate a mechanical failsafe design. The control electronics circuitry provides automatic tracking of the blade passage frequency. Results of laboratory, environmental and ground vibration tests employing an XH-51A stripped down helicopter fuselage show that the active cabin isolator reduces the vertical vibrations transmitted from the fuselage attachment point to the cabin attachment point at 18 and 36 Hz (or as an alternative, 6 Hz) by better than 90 percent. Notches of isolation at these frequencies automatically track changes in rotor rpm up to ± 10 percent. Similar reduction of vertical vibration levels across the seat servoactuator at 18 and 36 Hz were measured. The maximum deflection across either servoactuator due to combined 2-1/2 g synthesized sustained acceleration and ± 1 g vibration at 18 Hz, was 0.045 inches (0.114 cm). Recommendations are made regarding additional testing prior to flight evaluation of either system on the XH-51N research helicopter.

SECTION 1: INTRODUCTION

Even though the modern helicopter has remarkable performance capabilities, it suffers from restrictive limitations in the form of poor ride qualities and reduced structural integrity. The high levels of rotor-induced vibratory forces result in severe fuselage accelerations. Since the rotor shaft speed is maintained between relatively narrow limits, the fuselage vibration environment is essentially one of discrete frequency excitations. Critical frequencies correspond to: the shaft speed (1/rev); the fundamental blade frequency (b/rev), where b is the number of blades; and integral multiples of the blade passage frequency (2b/rev, 3b/rev, etc.).

Excitations occur in the vertical and horizontal directions. In-flight measurements of the three-bladed XH-51 helicopter indicate, however, that the vibration levels experienced at the cabin in the horizontal plane are considerably lower than in the vertical direction [Ref. 1]. The vertical vibration power spectral density of the XH-51 helicopter is shown in Figure 1, as a function of frequency. Most of the energy is concentrated at the blade passage frequency (18 Hz) and its first higher harmonic (36 Hz). The vibration at 1/rev (6 Hz) results from unbalance in the rotor assembly. These forces can generally be reduced to relatively low levels by use of proper blade balancing techniques.

In order to reduce the vertical vibrations transmitted to the cabin of the XH-51 helicopter at 18 and 36 Hz, a soft passive spring was used by NASA to isolate the cabin from the fuselage [Ref. 2]. Test data from helicopter flights with the isolated and nonisolated cabin configurations indicated that although the passive system did provide a significant reduction in cabin vibration levels, the system had some undesirable characteristics. These included: mechanical-control coupling due to relative displacement between the cabin and the fuselage; amplification of low-frequency motions; and cabin bottoming in a high g maneuver with resulting loss of isolation.

Active isolation systems have been previously developed by BARRY to provide a high degree of vibration isolation and displacement control at low frequencies [Refs. 3, 4]. Therefore, an investigation was conducted to design,

build and test two active isolation systems for the XH-51 helicopter capable of providing vibration isolation compatible with that afforded by the passive spring without the associated bottoming problems.

Figure 2 shows a schematic representation of the active cabin isolator and active seat isolator for the XH-51 helicopter. The active cabin isolator consists of a hydraulic actuator located between the cabin and fuselage in the space previously used by the passive spring. The active seat isolator makes use of an existing helicopter seat and additional structures to locate a hydraulic actuator between the seat and the cabin floor. Acceleration and displacement transducers are located on the cabin actuator and on the seat structure for feedback control of the cabin and seat isolators. Both isolators make use of a common hydraulic power supply and servoamplifier of sufficient capacity and power to operate only one system at a time. Eventually flight tests will be conducted with each separate isolation configuration to investigate differences in fuselage response and pilot performance between isolating just the pilot (seat isolator) or the pilot/controls/instrument panel combination (cabin isolator) from the vibrations experienced at the cabin.

This report presents the analysis, design, laboratory and preliminary ground tests of both the active cabin and seat isolators. Section 2 deals with a detailed description of the various system components. A servo-analysis of the active cabin and seat isolation systems is shown in Section 3. Section 4 discusses the system failure modes and associated failsafe logic design. Results of the laboratory tests conducted at BARRY and preliminary ground tests conducted at NASA Langley Research Center are given in Section 5. Finally, Section 6 presents conclusions and recommendations based on the investigation reported herein.

SECTION 2: SYSTEM SPECIFICATIONS AND DESCRIPTIONS

Based on a total nominal design cabin load of 1,320 pounds (600 Kg) and the previously measured isolation performance provided by the 3.3 Hz passive spring, the design goals for the active cabin isolation system were established as follows:

1. At least 90 percent isolation of cabin response to the basic vertical rotor-induced frequency input (18 Hz), with the same degree of vertical isolation at one or two additional frequencies (6 and 36 Hz) if feasible.

2. Insensitivity to rotor speed variation of up to ± 10 percent.

3. Maximum vertical dynamic deflection of ± 1/4 inch during 2-1/2 g acceleration maneuvers.

4. Minimal modifications to existing helicopter frame.

5. Failsafe design.

Similar specifications were established for the active seat isolator, except for a maximum design supported load of 385 pounds (175 Kg).

Two separate fuselage configurations of the XH-51 helicopter were considered in the investigation. Figure 3 shows the airworthy XH-51N helicopter presently used by NASA Langley Research Center, as a flying laboratory for advanced research in the rotary-wing aircraft field. After successful completion of ground tests and flight worthiness evaluation, the cabin and seat isolators developed under the investigation reported on herein will be flight tested in this aircraft. Figure 4 shows the stripped down XH-51A helicopter used to insure proper matching of components and to conduct laboratory tests at BARRY and ground tests at NASA/LRC. Figure 5 shows the cabin separated from the fuselage and the bracket support used for attaching the actuator between the cabin and the fuselage. The isolation system was designed to be compatible with electrical power and spatial constraints of the airworthy XH-51N helicopter.

4

Hydraulic Power Supply

It was originally desired to locate two self-contained electrically-powered units behind the pilot's seat – each containing a hydraulic power supply and a servoamplifier, suitable for both ground and flight testing. These units would power and control separate hydraulic actuators to generate the required forces for isolating the seat and cabin, respectively. However, during initial design stages, it became apparent that a different approach was necessary.

In order to produce the hydraulic power needed to provide 90 percent isolation of the vertical forces transmitted to the cabin at 18 Hz would have required approximately 2000 VA of AC electrical power. Only 250 VA of 208/115 volt, 400 Hz, three-phase AC are available for this purpose on board the XH-51N helicopter. The XH-51N power plant has a provision for a hydraulic pump accessory drive capable of delivering up to 6 HP. Therefore, the isolation system was designed to incorporate this drive. Hydraulic power for the airborne system is supplied from an engine driven pump at 3 gpm (190 mℓ/sec) and 1500 psi (105.2 Kg/cm^2). All hydraulic components are in accordance with MIL-H-8775, "General Specification for Hydraulic System Components, Aircrafts and Missiles."

Because of the amount of heat to be dissipated (15,000 Btu/hr)(4.4 Kilowatt), a heat exchanger could not be located in the cabin but was designed to be an integral part of the port side transmission door. Hydraulic swivel joints were used to allow opening and closing the door during ground maintenance of the aircraft. Louvers are incorporated into the starboard side door to provide cool air flow through the transmission compartment. The airflow is boosted by a fan on the heat exchanger assembly, and is then exhausted from the exchanger to atmosphere through louvers on the port transmission door.

The remaining hydraulic power supply components were packaged together in one unit, identified as the Integrated Accessory Package (IAP), and located behind the pilot's seat (starboard). The IAP contains accumulators, filters, reservoir, boost pump, valves and switches required for operation. A block diagram of the various components of the hydraulic power supply is shown in Figure 6.

For ground testing of the isolation system, an Auxiliary Power Package (APP) was designed to provide hydraulic power which is not available when the helicopter engine is not running. The APP includes a pump which is equivalent to the engine driven pump but is powered by an electric motor.

Cabin Actuator

The existing cabin spring mounting assembly was modified to accept a hydraulic actuator. The actuator was designed to BARRY specifications and in accordance with MIL-C-5503, "General Requirements for Aeronautical Hydraulic Actuating Cylinders." The actuator design included an unequal area piston to reduce the size of the actuator necessary to support the static compressive cabin weight. The servovalve, mounted integral to the actuator, was designed with unequal flow gains to provide a linear velocity gain. A special lockout device was designed to hold the actuator in the fully retracted position for supply pressures below 300 psi (21 Kg/cm^2). The lockout provides a mechanically rigid, failsafe link when the actuator is retracted without pressure. Also built into the actuator are transducers for relative displacement and absolute acceleration.

The actuator is attached to the cabin and fuselage by aircraft bolts which pass laterally through spherical bearings in the rod end and tail-stock end of the actuator. The spherical bearings allow small pitch and roll motions to occur between the cabin and fuselage. Although these motions are constrained somewhat by the cabin linkage design, structural bending and linkage geometry allow enough motion to require the actuator to be free in all directions except vertical (axial).

When installed the actuator body is affixed to the cabin and the piston rod is affixed to the fuselage. In this way the accelerometer can be built into the actuator body. Also, during operation, the hydraulic hoses move with the actuator and the IAP on the cabin floor reducing the possibility of fatigue.

Seat Actuator

Pilot seat isolation is provided by a BARRY designed seat actuator frame assembly. The actuator design is conceptually the same as the cabin

6

actuator with respect to piston, servovalve, position transducer, and lockout design. However, the actuator is rigidly mounted in the frame assembly without motion bearings and the piston rod supports and moves the seat load along linear bearing rods. The accelerometer is mounted on the seat portion of the frame assembly to provide feedback.

The seat actuator frame assembly was designed to replace the basic support frame of the existing XH-51 helicopter seat. The actuator motion axis is aligned 13 degrees aft of the vertical axis in order to accommodate the seat structure with minimum space loss. The active seat is located in the starboard cabin position. However, only cabling and plumbing changes are necessary to mount it in the copilot's position (port side).

Control Electronics Package

The electronics for servo control of the cabin and seat actuators and of the power supply are contained in a specially designed control electronics package (hereon referred to as the servoamplifier) mounted to an instrumentation table behind the starboard pilot seat. Either, but not both, the cabin actuator or the seat actuator can be connected into the servoamplifier and power supply. The gains and connections are compatible. Also included with the servoamplifier is a pilot control box, which allows the pilot to control the system mode of operation at his console. It also provides control to the operator outside the aircraft during ground testing.

Table I shows a summary of component specifications and system power requirements. Photographs of the cabin actuator, IAP, servoamplifier, seat actuator assembly, heat exchanger assembly, and APP are shown in Figures 7 through 11, respectively.

SECTION 3: SERVO ANALYSIS

This section presents a simplified servo analysis of the cabin and seat active isolation system for the XH-51 helicopter in the various operating modes. No attempt was made to simulate all of the complex dynamics associated with the fuselage and cabin structures. Instead, the helicopter was simulated by a simplified lumped parameter model. On this basis, an evaluation was made of the effect rigid body resonances would have on system performance.

Figure 12 shows a block diagram of the active system applicable to both the cabin and seat isolators. There are four modes of operation that the system can be in:

1. Locked Out Mode (Stop Mode)

   In this mode the bypass valve prevents pressure build-up, and the actuator mechanical lockout device engages. This mode occurs before power is brought up, and during the manual or failsafe stop mode.

2. Standby Mode

   In this mode the system is held hydraulically at the actuator null by the position loop.

3. Isolate Mode

   In this mode the position and acceleration feedback loops combine to provide isolation about the actuator null. Isolation frequencies are set by a tachometer tracking circuit.

4. Phase Lock Mode

   In this mode the tachometer signal is aided by a phase sensing feedback loop.

During the laboratory tests, the active system was energized to provide notches of isolation at 18 and 36 Hz, simultaneously. System parameters were changed during ground vibration tests to provide isolation at these same frequencies or at 6 and 18 Hz, simultaneously.

Standby Mode

In the Standby Mode the isolation relays open the acceleration feedback loop. The velocity gains K_{VD}/A for the cabin and seat actuators are 0.41 (1.04) and 0.37 (0.94) in./sec/ma (cm/sec/ma), respectively. These values are used as a combined gain term for the servoactuators since the area and flow rates are different for retraction and extension. The ratio of flow rate to area is equal in both directions. The displacement input is calibrated at 10.8 volt/in. (4.25 volt/cm). Combining the electrical gains of the position loop with the above mechanical gains yields the following expression:

$$\text{Position loop gain} = K_5 K_6 K_{VD}\left(\frac{K_Q}{A}\right) \tag{3-1}$$

Using the values of gain given in Figure 12 and Equation (3-1), the position loop unity gain crossover point can be calculated to occur at 22.1 $\sec^{-1}$ or 3.5 Hz. The valve dynamics can be ignored since they occur above 100 Hz. Therefore, in the Standby Mode the system behaves as a Type I integral position control system, with a transmissibility across the actuator of unity.

Isolation Mode

In the Isolation Mode the isolation relays close the acceleration feedback loop through the notch filter functions. These functions are:

$$\text{Notch Filter Function} = \frac{\tau_N s}{\left(1 + \tau_N s\right)^2 \left(1 + \tau_N^2 s^2\right)} \tag{3-2}$$

The time constants for these functions, τ_N, correspond to 18 Hz and 36 Hz for the b/rev and 2b/rev notches, respectively. The bandpass of the position loop is one-fifth of the b/rev frequency and one-tenth of the 2b/rev frequency, and can be ignored in the stability analysis. The servovalve dynamics can also be ignored. The seat servovalve dynamics are quadratic at 250 Hz with a damping ratio of 0.8. The cabin servovalve dynamics are quadratic at 160 Hz with a damping ratio of 0.8. The acceleration input has been calibrated at 2.0 volt/g.

The broad-band acceleration gain is given by

$$\text{Broad-band Acceleration Gain} = K_{bb}\tau_N$$

$$= K_1 K_2 K_{VD}\left(\frac{K_Q}{A}\right) \qquad (3\text{-}3)$$

Using values given in Figure 12 and Equation (3-3) the broad-band acceleration gain is calculated to be approximately $0.5\tau_N$ with a phase of +90 degrees for both the b/rev and 2b/rev loops. The gain is directly proportional to frequency with a unity gain crossover point at 38.4 Hz for the b/rev loop and 76.8 Hz for the 2b/rev loop, respectively.

The total acceleration loop dynamics can be described by:

$$\text{Total Acceleration Loop Dynamics} = \sum_{N=1}^{2} \frac{0.47\tau_N^2 s^2}{\left(1+\tau_N s\right)^2 \left(1+\tau_N^2 s^2\right)} \qquad (3\text{-}4)$$

Both of the notch functions have second order differentiations before the notch frequency, and second order lag functions after the notch frequency. At the mean frequency between the two notch functions the gain in each notch is approximately 0.235; the phase of the b/rev notch is near -110 degrees while the phase of the 2b/rev notch is near +110 degrees. Therefore, at the mean frequency the two loops subtract and result in very low acceleration loop gains. With very low gains at the mean frequency the closed loop behaves as in the Standby Mode, and the transmissibility approaches unity. Also, for purposes of the simplified closed loop analysis, the notches can be assumed to act independent of each other.

A simplified block diagram for a single notch isolation system can be represented by:
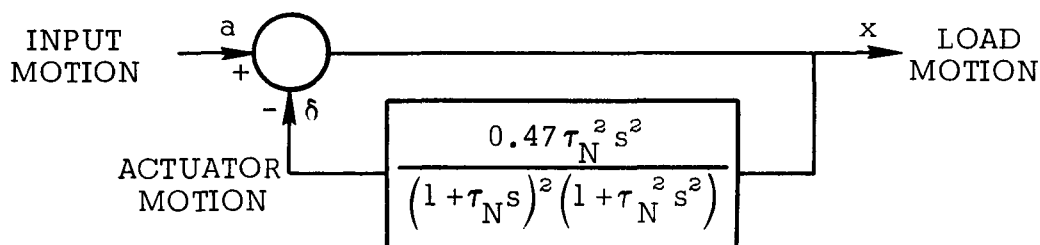
The closed loop transfer function between load motion and input motion is given by

$$\frac{x}{a} = \frac{\left(1 + \tau_N s\right)^2 \left(1 + \tau_N^{\ 2} s^2\right)}{\left(1 + \tau_N s\right)^2 \left(1 + \tau_N^{\ 2} s^2\right) + 0.47\,\tau_N^{\ 2} s^2} \qquad (3-5)$$

or

$$\frac{x}{a} = \frac{\left(1 + 2\tau_N s + \tau_N^{\ 2} s^2\right)\left(1 + \tau_N^{\ 2} s^2\right)}{\left[1 + 2(0.869)\tau_N s + \tau_N^{\ 2} s^2\right]\left[1 + 2(0.136)\tau s + \tau_N^{\ 2} s^2\right]} \qquad (3-6)$$

The first quadratic in the numerator nearly cancels the first quadratic in the denominator so that the closed loop transmissibility can be approximated by

$$\text{Transmissibility} \quad \frac{x}{a} = \frac{\left(1 + \tau_N^{\ 2} s^2\right)}{\left[1 + 2(0.136)\tau_N s + \tau_N^{\ 2} s^2\right]} \qquad (3-7)$$

Due to the quadratic functions, the resultant transfer function is a very narrow notch function at the frequency corresponding to τ_N. To provide ninety percent isolation at the notch frequency, it is only necessary to produce a numerator quadratic with a damping ratio of 0.0136. With the electronics of the system it is possible to produce a quadratic with 0.001 damping ratio with very little effort. Such a margin compensates for drift and nonlinearities of the electronics.

Tachometer Tracking

A very narrow notch can present problems if the input frequency varies from the notch frequency. The variation of shaft rotational speed can be as much as ten percent. Such a variation could mean a 1.8 Hz mismatch between input frequency and the b/rev notch frequency with a resulting complete loss of isolation. To overcome this problem the system is equipped with a tachometer input signal.

The tachometer input signal is directly proportional to rotor speed. A ten percent variation in speed results in a ten percent variation in tachometer

input signal. The tachometer input signal is fed into the two notch circuits and squared. The frequency of each notch is then directly proportional to rotor speed. A change in rotor speed will result in a proportional change in input vibration frequency and notch frequency. In this way, the narrow notch assures that the desired isolation of the input vibration is attained.

Phase Lock

A preliminary analysis of the response of the fuselage with an active cabin isolation system predicted the possibility of rigid body resonances of the helicopter occurring near the frequencies to be isolated. An analog computer representation of the simplified four-mass model shown in Figure 13 was used to calculate the open loop transfer function for the b/rev notch shown in Figure 14. As indicated in Figure 15, a structural resonance condition occurring at 14.5 Hz, results in a loss of isolation.

To provide isolation with such resonances, it is necessary to design a very narrow notch of isolation. As a function of broad-band gain the transmissibility is given by

$$\frac{x}{a} = \frac{\left(1 + \tau_N s\right)^2 \left(1 + \tau_N^2 s^2\right)}{\left(1 + \tau_N s\right)^2 \left(1 + \tau_N^2 s^2\right) + K_{bb} \tau_N^2 s^2} \qquad (3-8)$$

As the broad-band gain is decreased the notch becomes narrower and narrower. In the limit

$$\lim_{K_{bb} \to 0} \frac{x}{a} = 1 \quad \text{for } s \neq j/\tau_N \qquad (3-9)$$

and

$$\lim_{K_{bb} \to 0} \frac{x}{a} = 0 \quad \text{for } s = j/\tau_N \qquad (3-10)$$

In other words, isolation can be had at the expense of notch width and broad-band gain. To provide stability through rigid body resonances it was necessary to reduce broad-band gain resulting in a very narrow notch. The tachometer tracking notch provides 90 percent isolation with a bandwidth

12

of 0.2 Hz at the b/rev frequency. A reduction in gain by four will result in a notch bandwidth on the order of 0.05 Hz. The tachometer variance is ±1.8 Hz. The notch bandwidth would then be only 1.4 percent of the tachometer variance. For good isolation the tachometer would have to be accurate to 1 percent. This was felt to be unreasonable.

To overcome this problem, the system includes a means of determining the difference between the input frequency and the notch frequency. As indicated in Figure 16, this difference is summed with the tachometer signal and drives the notch frequency to the input frequency. In so doing, the desired isolation is obtained. The frequency difference is determined by the phase across the notch quadratic. The phase of a quadratic without damping switches from zero degrees to 180 degrees right at the notch frequency. Using this phase signal in a closed loop around the notch, the notch will lock onto the input frequency. The resulting phase lock notch aids the tachometer signal in providing 90 percent isolation. The phase lock is limited to a range of ± 0.5 Hz from the b/rev frequency as determined by the tachometer tracking signal.

Because the phase lock notch uses the instantaneous acceleration signal after filtration at the notch control frequency, it is relatively insensitive to acceleration noise at other frequencies. Nevertheless, if noise is present, the degree of isolation afforded with phase lock can be lower than that provided without phase lock. Therefore, to determine the effect of noise in a particular airborne environment, the best isolation attained with phase lock should be compared to the best isolation without phase lock.

SECTION 4: FAILURE ANALYSIS

This section discusses the failsafe philosophy and approach applied to the XH-51 active cabin and seat isolation system. Figure 17 shows the reference block diagram for the failure logic. The failures can be classified into three groups: manual, power, and operational. Manual failure results from interruption of system operation by the pilot. Power failure is the loss of electrical or hydraulic power. Operational failures occur when the system exceeds any predetermined limit of acceleration velocity or displacement. The failsafe design was predicated by the flightworthy and man-rating requirements of the system.

Manual Failure

The pilot has direct access to the solenoid valve in the hydraulic system. The solenoid valve must be picked (drawing power) in order to build pressure to 1500 psi. The stop switches are wired in series with the solenoid valve. In this way the pilot has direct control of hydraulic power. Should the system fail, and the automatic failure circuits fail, the pilot has the ability to shut off hydraulic power. When hydraulic power is off, the actuator will not be capable of supporting the load and it will retract. After complete retraction the lockout mechanism will hold the actuator retracted as a rigid link. The lockout assures that if the acceleration of the load exceeds gravity, no cavitation of the actuator will occur. Once hydraulic pressure has been removed the system is mechanically in a failsafe mode.

Should the system be operating normally without failure, the transfer of the stop switch would place the system in the Stop Mode. The Stop Mode relay controls an SLND relay and a sequence control relay. An SLND relay contact is wired in series with the solenoid valve. This contact opens when the stop relay is picked and drops the solenoid valve. The SLND relay contact is used for automatic failure and shutdown of the system. It is redundant to the stop switch function under manual stop.

The sequence control relay opens the feedback loops at the valve driver amplifier. Initially it nulls the servovalve. A gradually increasing signal then commands the actuator to go down. This nulling and gradually

increasing down command assures that no harsh transient condition occurs during the stop sequence. When the system is started, the start relay interrupts power to the operational failsafe relays, the stop relay and the main isolation relay. When the stop relay and main isolation relay drop, they in turn drop the sequence control, SLND and individual isolation relays. As a result, when the system is in the Start Mode all relays are dropped by the start relay. The start relay is held up by a discharging capacitor for approximately 10 seconds. During this time, the hydraulic pressure builds up and the down command on the servovalve from sequence control gradually decreases. By the time the start relay drops the system reaches a position null and all operational failure circuits are reset. The gradual decrease of the servovalve down command assures that no harsh transient occurs during the start sequence.

<div align="center">Power Failure</div>

Three possible losses of power can occur. The +28 volt DC circuit breaker could throw, or a power lead could open. The AC circuit breaker could throw, or a power lead could open. The hydraulic system could malfunction.

In the event that +28 volt DC power is lost, the solenoid valve would open, dropping hydraulic pressure. The solenoid valve is a normally open valve. It requires 1.5 amps of DC power to close the valve. Since a loss of DC power would cause the valve to become normally open, the valve is failsafe. Loss of DC power would also cause the isolation relays to open, placing the system in the Standby Mode. The system would stay in the Standby Mode and slowly drift to the bottom as hydraulic power decreases. The system would not fail under sequence control since DC power is necessary for the operation of the sequence control and stop relays. No harsh transient will occur with this type of failure. The servovalve is always in the closed loop and only loses its effectivity as pressure drops.

In the event of a loss of AC power, the boost pump in the IAP would stop. This would cause a drop in boost pressure transferring the boost pressure switch. This, in turn, would pick the stop relay and drop the

solenoid valve. Loss of AC power would make the sequence control inoperable and the shutdown transient is not readily predictable. Most likely, the loss of AC power will result in loss of valve driver power and constant nulling of the servovalve. The weight of the load would then cause the actuator to retract slowly.

There are five hydraulic malfunctions that will result in automatic failsafe shutdown under sequence control. They are:

(a) Low boost pump output pressure (< 15 psi)(<1.05 Kg/cm^2)

(b) High system pressure (> 1900 psi) (> 133.5 Kg/cm^2)

(c) High hydraulic fluid temperature (> 160° F)(>71.1° C)

(d) Excess pressure drop across the main filter
(> 75 psi) (> 5.25 Kg/cm^2)

(e) Overheated auxiliary pump.

A series of switches operated by these conditions control the hydraulic fail-safe relay. This relay, in turn, picks the stop relay and results in controlled shutdown. A loss of oil through leakage would eventually result in starving the boost pump and causing a low boost pressure failure.

Operational Failure

The system is capable of automatic shutdown under four operating failure conditions:

(a) Greater than 2 g acceleration vibration in the Isolation Mode.

(b) Greater than 10 percent of the flow corresponding to 1 g at 18 Hz in the Standby Mode.

(c) In the Isolation Mode the same as (b), except for flow components in the 18 Hz and 36 Hz frequency bands.

(d) Greater than 0.15 inch (0.381 cm) deflection from actuator null.

These conditions are sensed and, when they are exceeded, the respective failsafe relay picks the stop relay, after which controlled shutdown occurs.

SECTION 5: EXPERIMENTAL RESULTS

Tests were conducted at both BARRY and NASA Langley Research Center including environmental tests, laboratory performance checkout tests, and ground testing of the active cabin and seat isolation system installed on the XH-51A fuselage.

Environmental Tests

Although the XH-51N helicopter is a research aircraft, all components were tested for satisfactory performance while being subjected to induced environments associated with more stringent military operation. The specific tests consisted of:

1. Vibration Cycling per MIL-STD-810, Method 5.4, Procedure I, Part 3.
2. Shock per MIL-STD-810, Method 516, Procedure I.
3. Explosion Proof per MIL-STD-202, Method 109.
4. Electromagnetic Interference per MIL-STD-461, Class IIB.

All of the equipment performed satisfactorily to these tests.

During vibration testing the servoamplifier exhibited a vertical resonance at 18 Hz. BARRY 2K-2 isolation mounts were used to provide a 10 Hz resonance and avoid coupling with the helicopter b/rev frequency.

During vibration testing of the seat under MIL-STD-810 inputs, a lateral resonance at 26 Hz, apparently caused by the bearing guide rods, was observed. No modification of the seat structure was undertaken, however, for two reasons. First, the mounting configuration of the seat during the laboratory test (directly to the shaker) is not representative of the actual installation on the aircraft; and, second, flight test records do not indicate any 26 Hz component on the cabin response which would excite this particular lateral mode of the seat structure.

Laboratory Performance Checkout Tests

Laboratory tests were conducted at BARRY to measure the open and closed loop response of the active seat isolation system. The open loop response of the active seat is shown in Figure 18. The transfer function across the actuator for the 2b/rev broad-band function with the position loop closed is

also shown. All responses are measured across the actuator and involve as little structure as possible. The 2b/rev broad-band function verifies the assumption of neglecting the servovalve dynamics. The total open loop transfer function also verifies the negligible effect the two notches have on each other.

The closed loop response of the active seat was measured on an electrodynamic shaker with an input of 0.5 g to determine the seat's axial transmissibility characteristics under various conditions. These included: Locked Out Mode; Standby Mode; Isolate Mode; Isolate Mode with tracking; Isolate Mode with phase lock notches; and Isolate Mode with tracking and phase lock notches. In all cases tests were conducted with no load on the seat and with 120 pound (54.5Kg) supported by a cushion. As indicated in Figures 19 through 23 the active seat response is independent of load.

Figure 19 shows the vertical transmissibility of the seat in the Locked Out Mode. Figure 20 shows the vertical transmissibility of the seat in the Standby Mode indicating a value of approximately 1 from 10 to 100 Hz. The two notches of isolation at 18 and 36 Hz are shown in Figure 21 for the condition of plain isolation without tracking. Figure 22 shows the transmissibility of the seat for the case of tachometer tracking. Data points in this curve were obtained by sinusoidal excitation and notch tracking of the shaker excitation frequency. The actual vibration response of the tracking notch would be that of the plain isolation condition (Figure 21) with the notches occurring at frequencies other than shown to satisfy the tachometer signal.

In Figures 21 and 22 the transmissibility exceeds unity at frequencies outside the notch frequencies. This is due to the fact that the isolation response of the system is more nearly represented by Equation (3-6) than by Equation (3-7). The quadratic in the denominator of Equation (3-6) is not entirely cancelled by the quadratic in the numerator, resulting in amplification.

Figure 23 shows the seat transmissibility for the phase lock condition. Upon first inspection the isolation provided by the phase lock notch (Figure 23) appears to be the same as that provided by the plain notch (Figure 21). In order to differentiate between them, the seat transmissibility in the neighborhood of the b/rev notch frequency is replotted on Figure 24 for both conditions.

It can be seen that the phase lock notch provides a 90 percent isolation bandwidth three times greater than the plain notch. Finally, Figure 25 shows the transmissibility of the seat for the case of tachometer tracking with the phase lock notches.

The advantage of the phase lock is that it results in a very narrow band of isolation at only the notch frequency. The narrow-band effect allows for a low broad-band acceleration loop gain to be coupled with a high gain narrow-band notch. Frequency sensing inaccuracies are overcome by the closed loop phase lock frequency control of the notch. The phase lock controls frequency in the same manner that the position loop controls the actuator position. In the latter, the null pot is the input and commands the actuator to a position which satisfies the loop. In the former, the input frequency commands the notch frequency to do the same. The frequency matching response time of the phase lock notch is a function of the phase lock loop gain. The bandwidth of the phase lock notch is determined by the rated error of the frequency sensing circuits. The tachometer tracking signal only needs to be accurate enough to place the notch frequency within this rated error.

Figure 26 shows the ability of the active seat isolation system to provide vibration isolation during conditions of combined excitations. The combined acceleration excitation consists of a 2-1/2 g ramp-sustained acceleration, trace (a), generated by a synthesis technique [Ref. 3], and a ± 1 g amplitude vibration at 18 Hz, trace (b), generated by an electrodynamic shaker. The degree of vibration isolation of the vibratory excitation (90 percent) is indicated in trace (c), which shows the acceleration response of the active seat measured at the servoaccelerometer. Trace (d) indicates the relative displacement across the actuator. At the onset of the sustained acceleration the maximum displacement reaches 0.045 inches (0.114 cm) and within 0.1 seconds it settles to ± 0.02 inches (0.05 cm).

Ground Testing

Ground tests were conducted at NASA Langley Research Center to evaluate performance of the active cabin and seat isolation system, and to identify the effect of the active system on the overall response of the helicopter fuselage.

The stripped down XH-51A fuselage was used for ground vibration testing. The test installation is shown in Figure 27. The helicopter was hung by elastic cords attached to a simulated rotor shaft. The primary vertical resonance of the suspension and helicopter was near 1.0 Hz. Engine and equipment inertias were simulated by lead masses distributed throughout the aircraft. A hydraulic shaker was rigidly fixed to the simulated rotor shaft with the shaker body capable of relative motion to the fuselage. Lead masses were attached to the shaker to simulate the rotor inertia. The static load of the shaker and lead masses was supported by elastic cords attached to the building structure.

The helicopter was instrumented with accelerometers and shaker controls. The instruments provided input vibration energy control and acceleration monitoring throughout the aircraft. During the initial phases of the ground testing, structural resonances in the helicopter and shaker setup produced noise accelerations greater than the controlled accelerations. To eliminate the effect of the noise accelerations a low frequency notch was implemented. The 2b/rev circuits in the isolation system servoamplifier were used with the notch frequency set at 6Hz.

Tests were conducted by sweeping the shaker frequency from 1 to 50 Hz and maintaining a controlled acceleration at the fuselage. The two available notch circuits in the servoamplifier were used to provide notches of isolation at 6 and 18 Hz (1/rev and b/rev), simultaneously, and at 18 and 36 Hz (b/rev and 2b/rev), simultaneously. The tracking notch was used during preliminary ground tests, but no data was recorded. In all cases the response of the active system was evaluated based on the ratio of acceleration measured with the system in the Isolate Mode to that measured with the system in the Standby Mode.

Figures 28, 29, and 30, respectively, show: (a) the open loop of the active cabin isolation system measured across the cabin actuator; (b) the ratio of acceleration measured at the cabin actuator servoaccelerometer with the system in the Isolate Mode, to the acceleration measured with the system in the Standby Mode; and (c) the ratio of the acceleration measured at the seat actuator servoaccelerometer with the system in the Isolate Mode to that measured with the system in the Standby Mode.

The various structural modes between the cabin and fuselage can be identified from the b/rev Broad-Band Open Loop Response curves in Figure 28. Compared to Figure 14, it can be seen that the measured structural mode occurring between 9 and 15 Hz is in agreement with the prediction made based on the simplified four-mass model used in the preliminary analysis. The open loop relative broad-band gain for the cabin K_{bb} is 0.1, which is approximately one-fifth of the value given in Equation (3-4). The measured response is closely approximated by Equation (3-7), resulting in very narrow notches of isolation. Also, as shown in Figure 29 the transmissibility does not significantly exceed unity. The very narrow notches and the low value of broad-band gain allow the system to be stable even though strong structural modes are present at frequencies near the notch frequency. In the case of the seat response, Figure 30, the peak transmissibility is higher than for the cabin isolator and the notches are wider due to the greater value of broad-band gain.

Discussion of Results

Results of the environmental, laboratory, and ground tests show that the active cabin and seat isolation system is capable of providing better than 90 percent isolation of vertical accelerations transmitted from the rotor through the fuselage to either the cabin or seat at the 1/rev, b/rev, and 2b/rev frequencies. The ability to: track changes in rotor speed; limit the relative displacement across the cabin actuator during sustained acceleration; and provide mechanical lockout have also been demonstrated.

As previously indicated the results of this investigation were intended not only to verify the feasibility of providing the required degree of vertical isolation and displacement control with an active system, but also to evaluate the flightworthiness of such a system for use with the XH-51N research helicopter. Several comments are worthy of consideration, particularly in regard to differences between the structural response of the XH-51A fuselage and the airworthy XH-51N, and to the nature of the actual vibration excitations experienced in flight.

The investigation reported herein is an initial step in a long-range program to provide a practical hardware solution to the problem of attenuating

multidirectional vibratory excitations experienced by helicopter crews. The particular short-range objectives of reducing the levels of vertical excitation at the cabin support and seat have been met. However, it should be emphasized that although 90 percent isolation, or better, was measured by the vertical accelerometers located at the actuators, the response of the cabin at other locations differed from that measured at the actuators. At the 1/rev frequency the same degree of isolation was provided throughout the cabin. The overall effect of the b/rev isolation on the cabin was good with the cabin isolator but not with the seat isolator. In either case, the effect of either the active cabin or seat isolator at 2b/rev was poor throughout the cabin. The degradation in isolation performance away from the actuator attachment points is due to: structural modes; load distribution within the aircraft; and characteristics of the mounting points. In order to evaluate the eventual use of the active system in the airworthy XH-51N helicopter, it is necessary to discuss the relationship of these items as tested in the XH-51A fuselage.

The ground test installation used to measure the previously shown results differs from the XH-51N in three significant ways: first, the XH-51N rotor mass is not rigid like the XH-51A shaker mass; second, the XH-51N rotor mass motion is not the same as the shaker piston; and third, the XH-51N transmission is isolated from the fuselage through a vibration mount while the XH-51A transmission is rigidly mounted. Therefore, the structural modes of the XH-51N will most likely be different from those found in the XH-51A.

The XH-51A ground test and laboratory shaker test data for the seat showed longitudinal and lateral structural modes. The loss of effective vertical isolation provided by the seat actuator in the XH-51A installation at the b/rev and 2b/rev frequencies was due to a compliant seat-to-cabin structural attachment point. When subjected to vertical vibrations on the shaker with a stiff attachment, the seat isolation system proved very effective. In this latter case, the shaker did not introduce in-plane vibration and no vertical or in-plane structural modes were excited. On the XH-51A fuselage, however, the seat exhibited longitudinal resonant motion at 18 Hz resulting in the loss of effective vertical isolation through the introduction of in-plane vibration. The attachment point of the seat on the XH-51A fuselage was the cabin main lateral beam. This beam is susceptible to torsional vibration

which result in longitudinal vibration of the seat. On the XH-51N the seat mounting configuration uses the cabin floor plate for attachment which may reduce (or, at least, change) the seat/cabin structural interaction.

Finally, during ground testing considerable rotational motions of the XH-51A cabin were noticed. It is questionable whether or not the stiffness of the links used during ground testing simulated those in the XH-51N cabin. Differences in the characteristics of the lateral and pitch links would result in considerable changes in the response of the cabin.

SECTION 6: CONCLUSIONS AND RECOMMENDATIONS

Conclusions

Conclusions based on results of the laboratory, environmental, and ground vibration tests conducted during this investigation are:

1. Electrohydraulic isolation systems can provide better than 90 percent reduction of the vertical forces transmitted from the fuselage to the cabin and from the cabin floor to the pilot seat structure at frequencies automatically tuned to the blade passage frequency b/rev (18 Hz), 1/rev (6 Hz), and 2b/rev (36 Hz).

2. Maximum vertical deflection across the servoactuators under combined simulated 2-1/2 g sustained acceleration and ± 1 g vibration at 18 Hz is 0.045 inches (0.114 cm).

Recommendations

The various tests conducted during this investigation show that the active cabin and seat isolation system is capable of providing the stipulated degree of vertical isolation and displacement control. However, in order to evaluate eventual use of the system on the airworthy XH-51N helicopter, further testing is recommended as a means to arrive at an understanding for, and achievement of, effective vibration isolation under flight conditions. The recommendations made below are based primarily on: (a) the anticipated differences between the structural response of the XH-51A fuselage used during ground testing and the airworthy XH-51N helicopter; and (b) on the complex nature of the actual vibratory excitations experienced in flight.

(1) It is recommended that the XH-51A cabin motions under ground vibration tests be studied to determine if bending is taking place in the cabin. If so, the various bending modes could be defined in order to evaluate whether or not they can be overcome. At present, the servoaccelerometer is located right at the cabin actuator. It may be possible to place the accelerometer at a more optimal location. Also, two accelerometers may provide feedback for two different notches. If this method is effective,

isolation could then be attained by simply relocating the control accelerometers.

(2) After arriving at a better understanding of the structural response of the XH-51A fuselage with the active cabin and seat isolation system, the XH-51N helicopter could be modified to accept the isolation system as finally installed in the ground tested XH-51A fuselage, whenever possible. It is not necessary that closed-loop ground vibration tests be conducted on the XH-51N helicopter. Only open loop tests would be required to determine stability and structural responses. If structural modes preclude stability, the aircraft could then be flown with the active cabin isolation system in the Standby and Locked Out Modes. Servoaccelerometer data would be recorded and analyzed for frequency content under different flight conditions. The frequency content of this data would determine the maximum possible isolation at the servo-actuator, and whether the 2b/rev notch should be converted to a 1/rev notch or some other frequency. The acceleration loops could finally be closed and isolation flight tests run.

REFERENCES

1. Clevenson, S. A.; Snyder, W. J.; and Catherines, J. J. : Preliminary
   Study of Effect of Vibration on Aircraft Ride Quality, NASA Aircraft
   Safety and Operating Problems LRC Conference, May 4-6, 1971,
   NASA SP-270.

2. Morris, Jr., C. E. K.; Ward, J. F.; Jenkins, Jr., J. L.; and Snyder, W.J.:
   Analysis of Some Helicopter Operating Problems, NASA Aircraft
   Safety and Operating Problems LRC Conference, May 4-6, 1971,
   NASA SP-270.

3. Calcaterra, P. C.; and Schubert, D. W. : Research on Active Vibration
   Isolation Techniques for Aircraft Pilot Protection, AMRL-TR-67-138,
   Aerospace Medical Research Laboratories, MRBAV, Wright-Patterson
   Air Force Base, Dayton, Ohio, 1967.

4. Schubert, D. W.; Pepi, J. S.; and Roman, F. E. : Investigation of the
   Vibration Isolation of Commercial Jet Transport Pilots During
   Turbulent Air Penetration, NASA CR-1560, July 1970.

TABLE I

SYSTEM SPECIFICATIONS AND POWER REQUIREMENTS

Cabin Actuator Area	Extend Retract	3.12 in^2 $(20.15$ cm$^2)$ 1.36 in^2 $(8.79$ cm$^2)$
Seat Actuator Area	Extend Retract	1.34 in^2 $(8.75$ cm$^2)$ 0.82 in^2 $(5.38$ cm$^2)$
Cabin Servovalve Rated Flow	Extend Retract	35.0 in^3/sec $(574$ cm^3/sec$)$ 17.5 in^3/sec $(287$ cm^3/sec$)$
Seat Servovalve Rated Flow	Extend Retract	14.2 in^3/sec $(232$ cm^3/sec$)$ 9.0 in^3/sec $(148$ cm^3/sec$)$
Engine Driven Pump	Rated Flow Input Power	11.5 in^3/sec $(139$ cm^3/sec$)$; 1500 psi $(105$ Kg/cm$^2)$ 50 in-lb $(1.67 \times 10^{-6}$ KW-hr$)$ at 7600 rpm
Auxiliary Pump/Motor	Rated Flow Input Power	11.5 in^3/sec $(189$ cm^3/sec$)$; 1500 psi $(105$ Kg/cm$^2)$ 11 amp. $208/120$ volt, 400 Hz, 3ϕ, AC
Airborne System (excluding pump)	Input Power	2 amp, $208/120$ volt, 400 Hz, 3ϕ, AC; 2 amp, $+28$ volt, DC
Heat Exchanger/Fan Capacity		$15,000$ Btu/hr $(4.4$ Kilowatt$)$
Vibration Isolation Levels		± 1.0g at 18 Hz; ± 0.5g at 36 Hz
Nominal Cabin Static Load		1320 lb $(600$ Kg$)$
Maximum Seat Static Load		385 lb $(175$ Kg$)$
Flow Required for Cabin Isolation	Max. Ave. Max. Peak	6.1 in^3/sec $(100$ cm^3/sec$)$ 13.3 in^3/sec $(218$ cm^3/sec$)$
Flow Required for Seat Isolation	Max. Ave. Max. Peak	2.94 in^3/sec $(48.2$ cm^3/sec$)$ 5.7 in^3/sec $(93.4$ cm^3/sec$)$
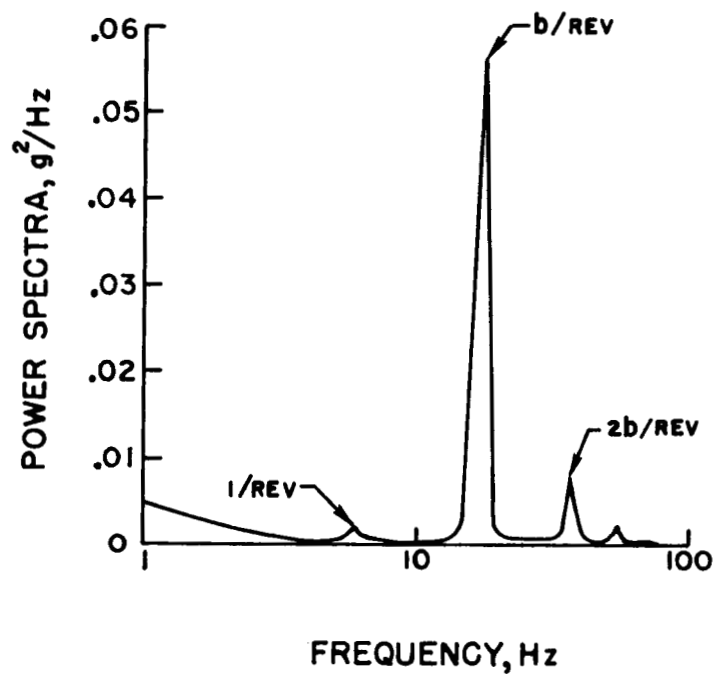
Figure 1: Power Spectrum of Vertical Vibrations Measured on XH-51N Helicopter at 130 Knots [Ref. 1]

CABIN

CABIN ISOLATOR

SEAT ISOLATOR

GUIDE LINKS

CONTROL SYSTEM
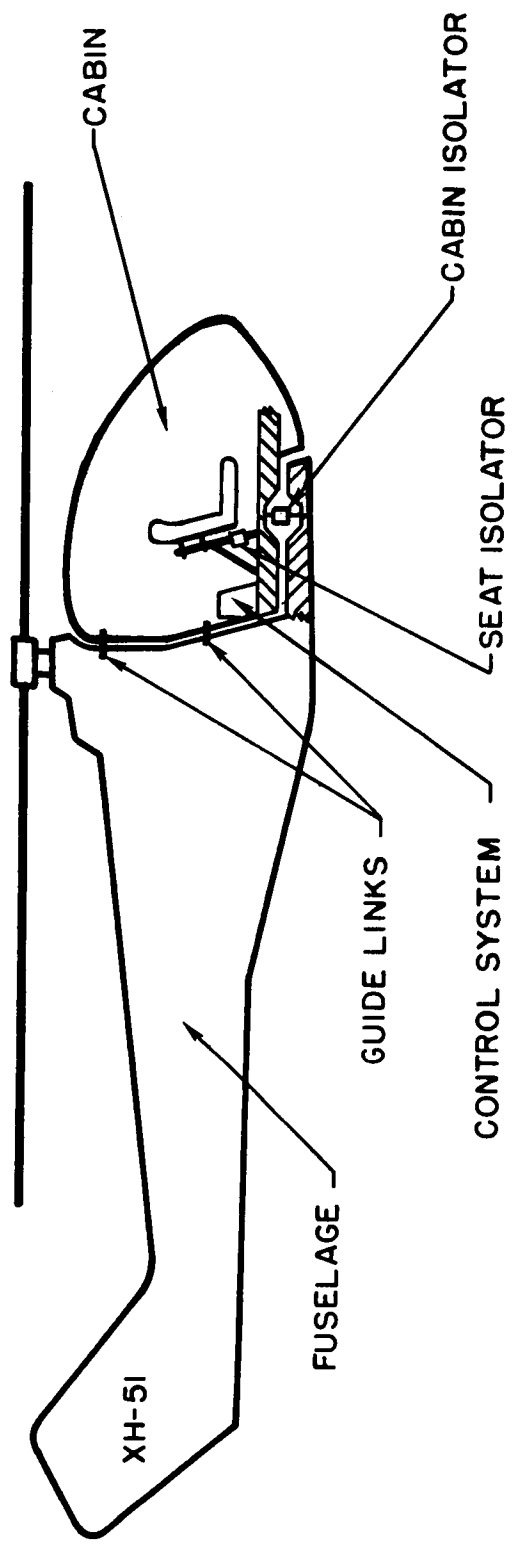
FUSELAGE

XH-51

Figure 2: Schematic of Active Cabin and Seat Isolation System
Installation on XH-51 Helicopter
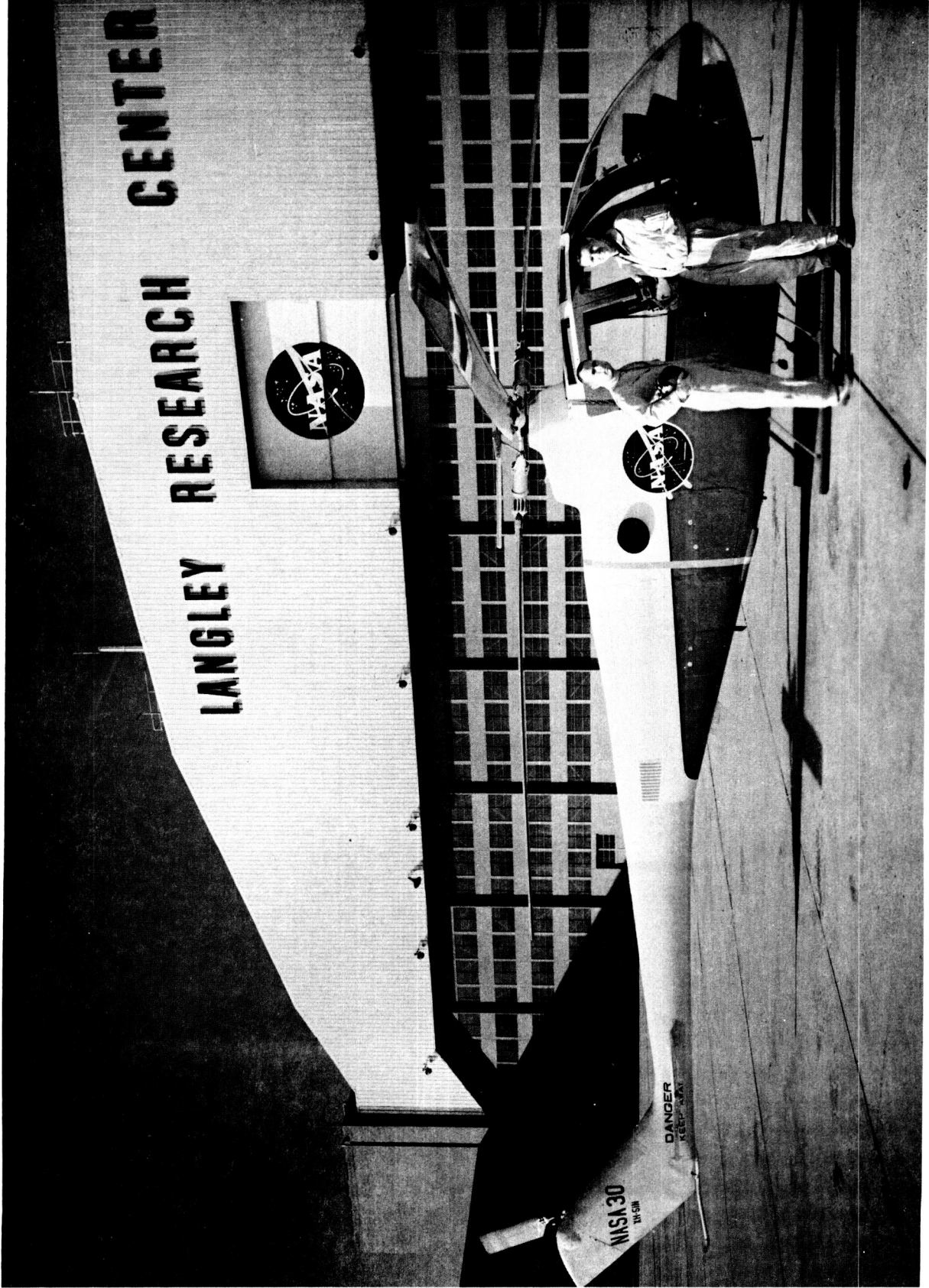
Figure 3: XH-51N Research Helicopter
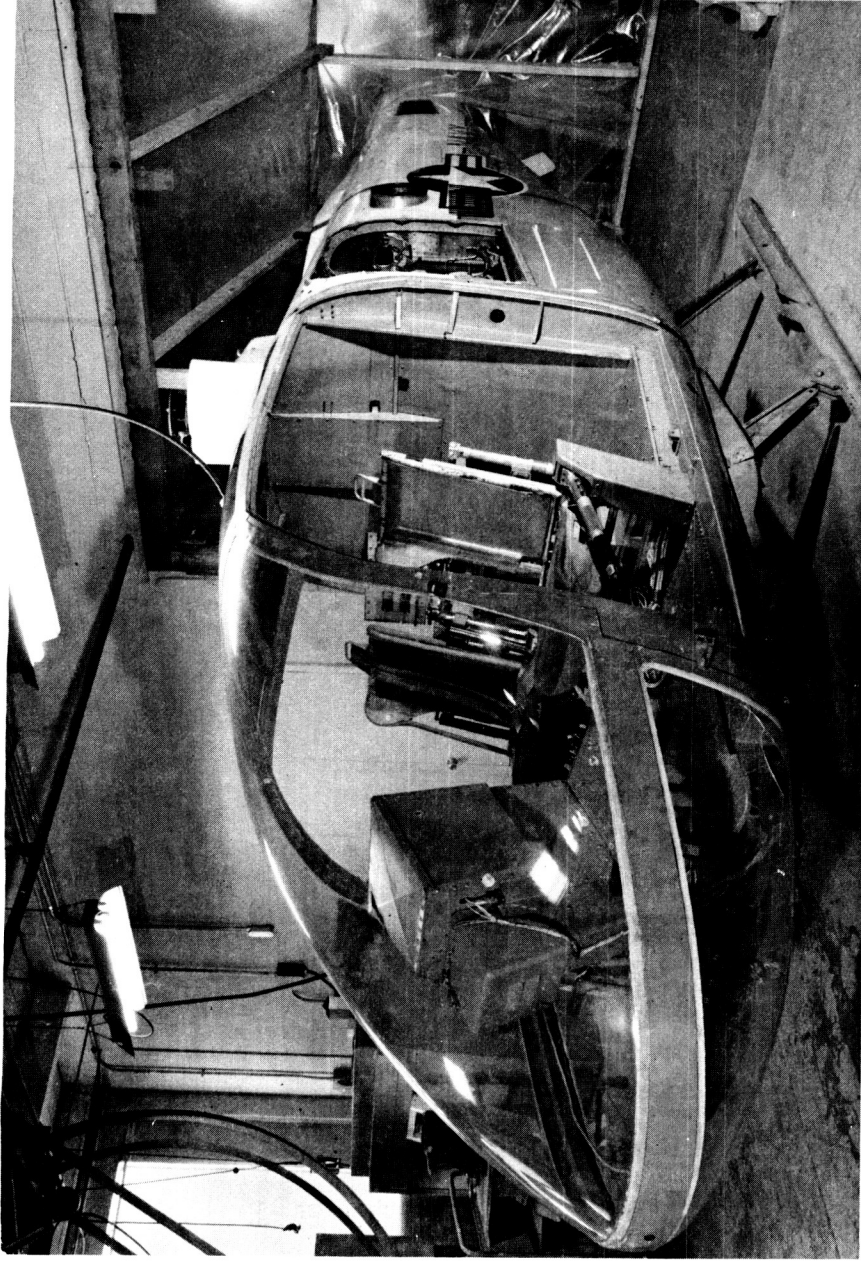
Figure 4: Stripped Down XH-51A Fuselage
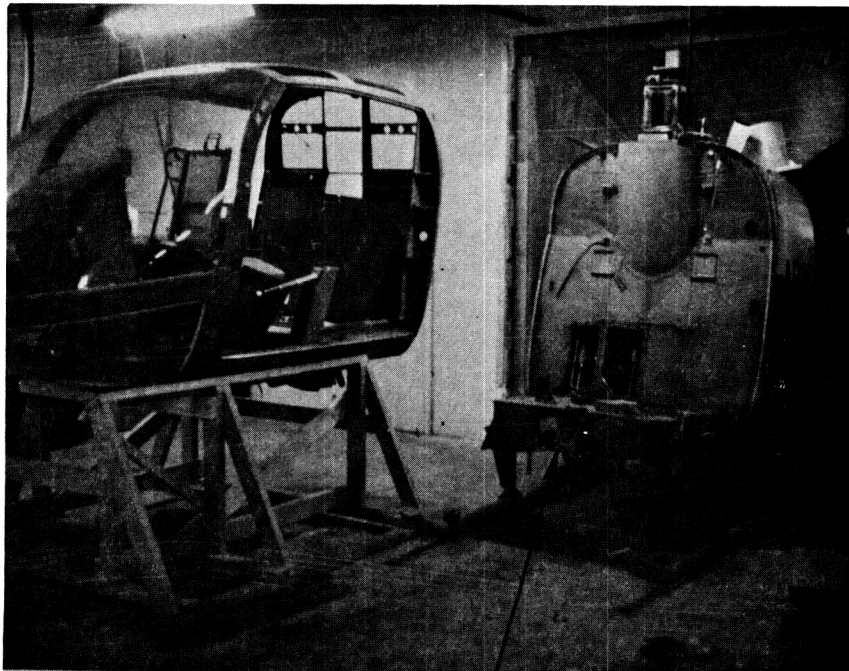
ACTUATOR
SUPPORT
BRACKET

Figure 5: XH-51A Cabin Separated from Fuselage
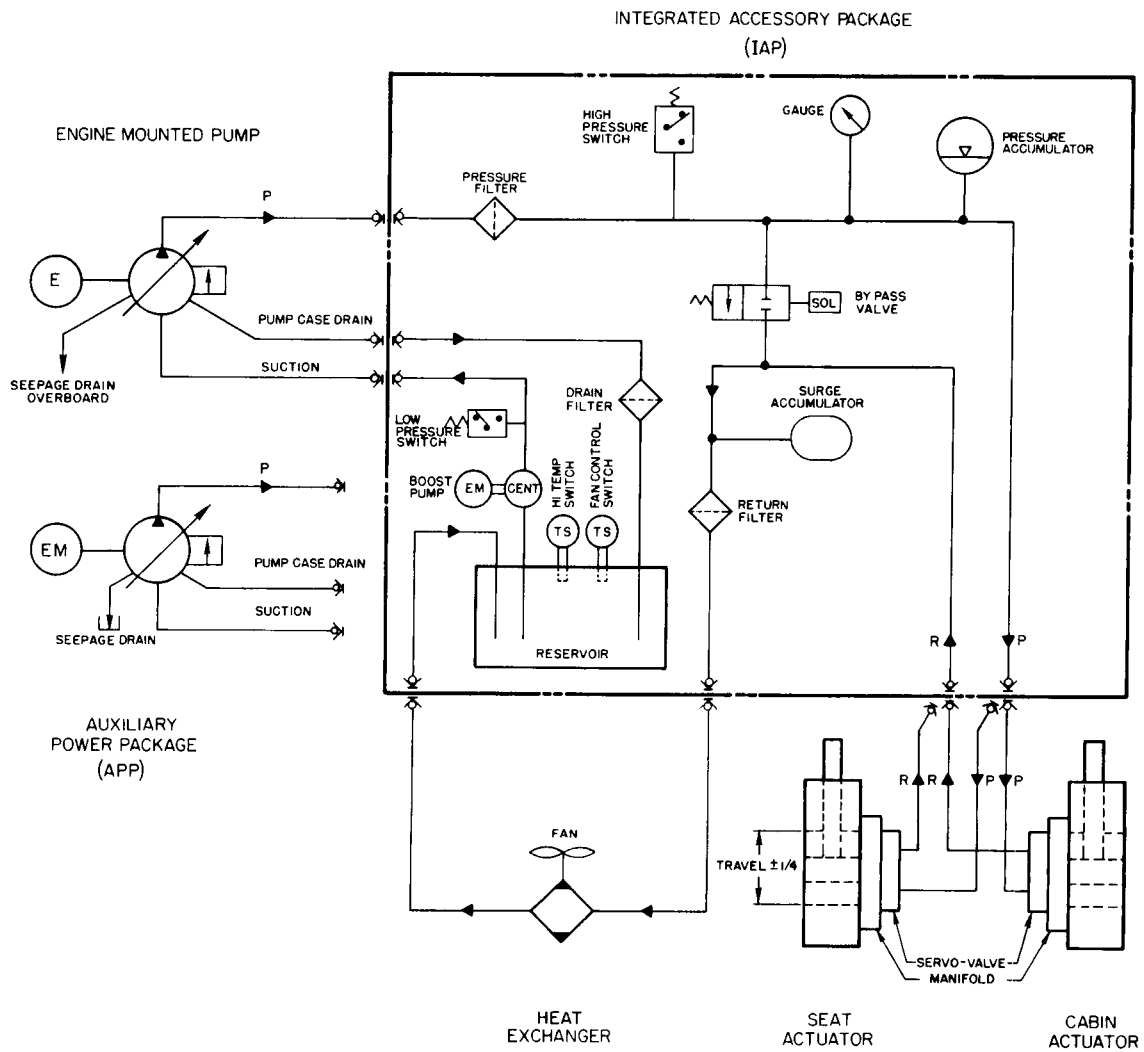
Figure 6: Block Diagram of Hydraulic Power Supply

CABIN
FLOOR

SERVOVALVE

ACTUATOR
MANIFOLD

ACCELEROMETER

ACTUATOR

FUSELAGE
SUPPORT
BRACKET
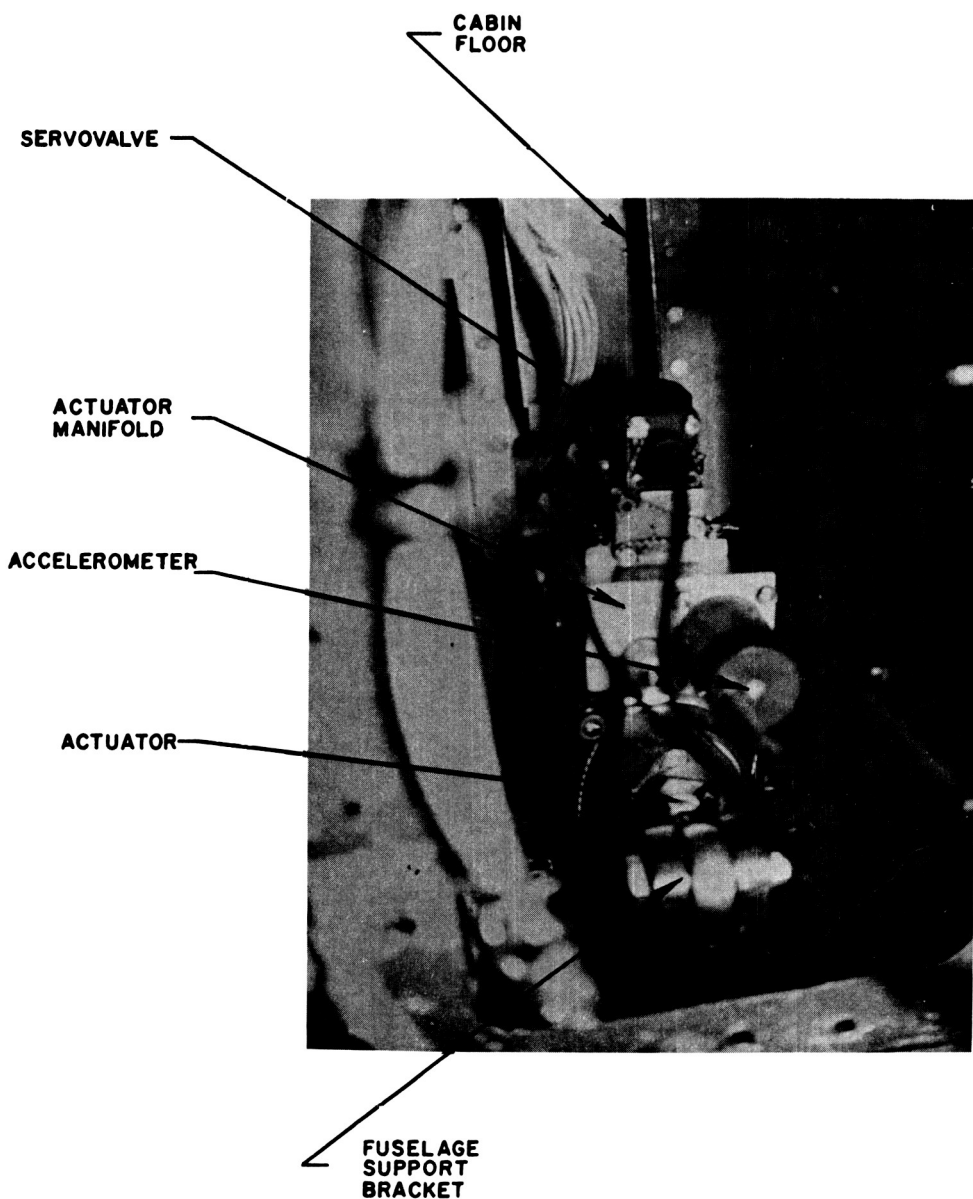
Figure 7: Active Cabin Servoactuator Installed in XH-51A Fuselage

CONTROL
ELECTRONICS
PACKAGE

INTERGRATED ACCESORY PACKAGE (IAP)

BEARING ROD
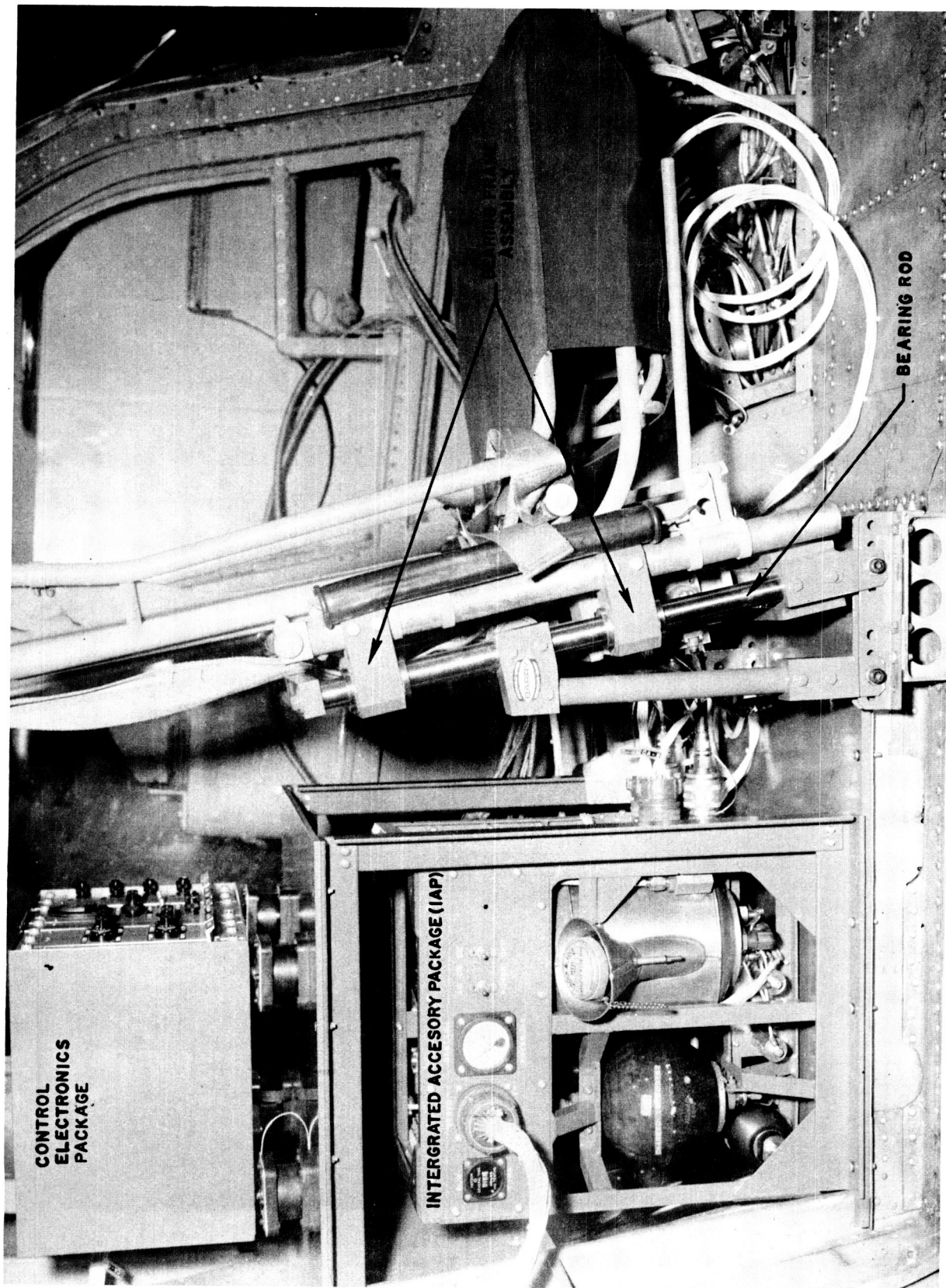
Figure 8: Integrated Accessory Package (IAP), Control Electronics Package and Active Seat Installed on XH-51A Fuselage
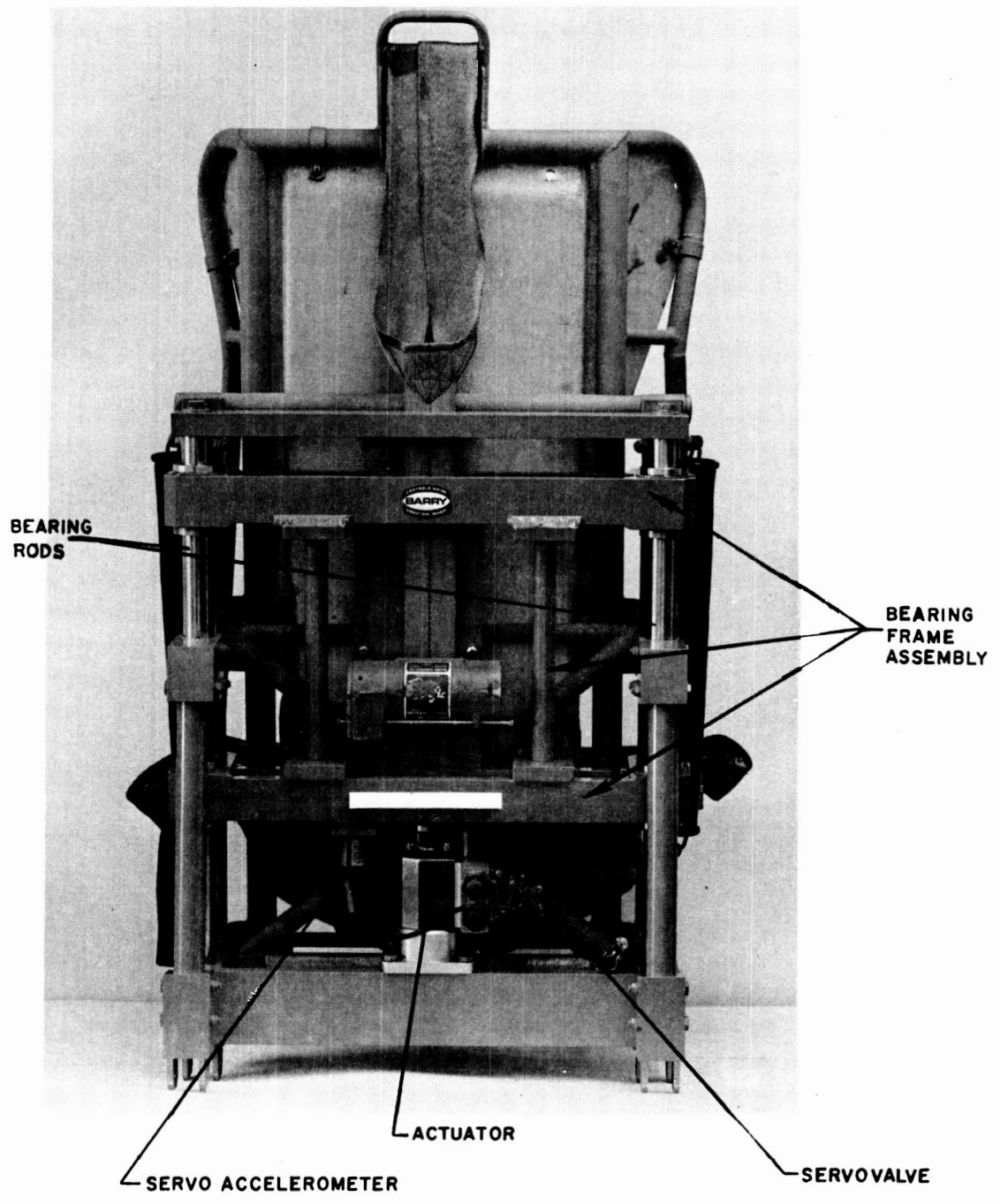
Figure 9: Active Seat Servoactuator Installation
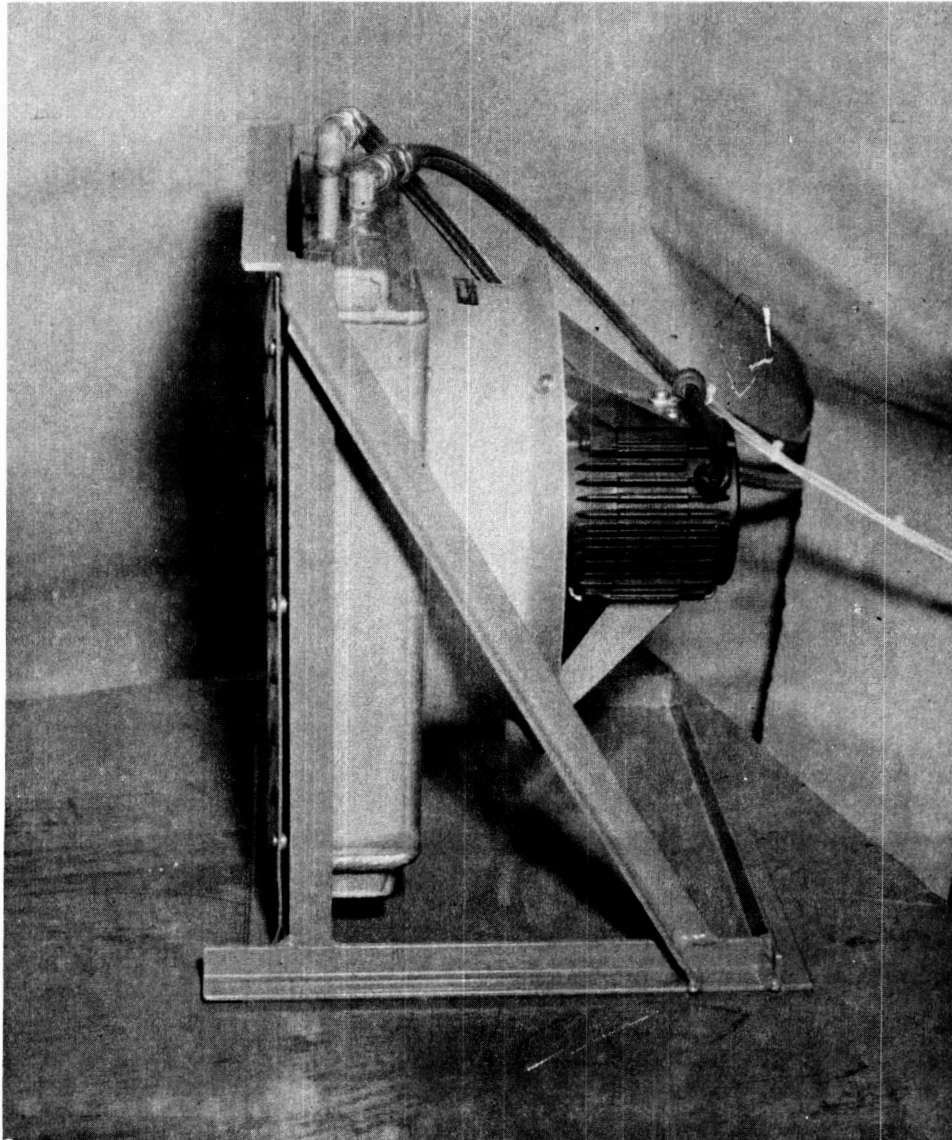
Figure 10: Heat Exchanger Assembly For Ground Testing
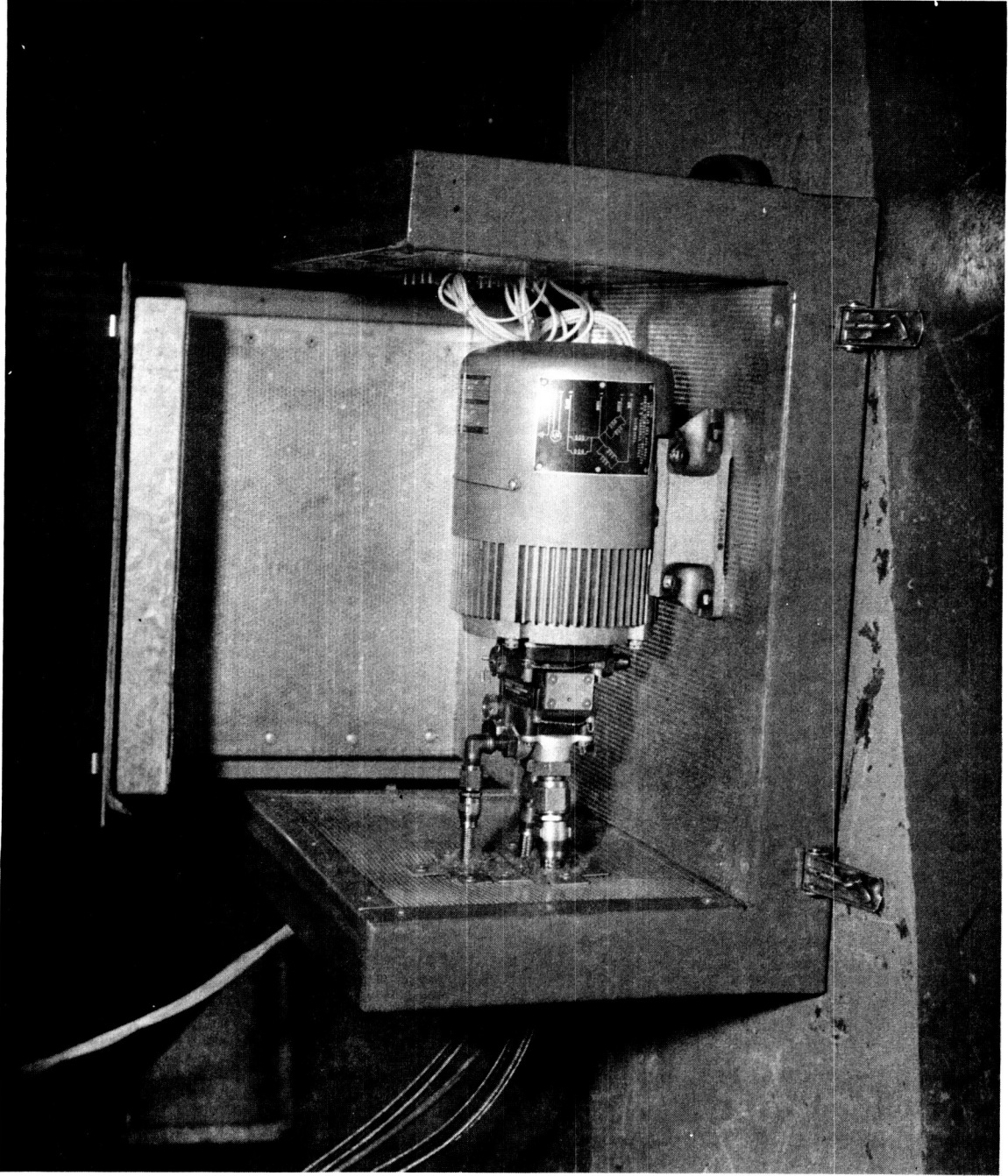
Figure 11: Auxiliary Power Package (APP) For Ground Support

Figure 12: Servo Block Diagram of Active Isolation System
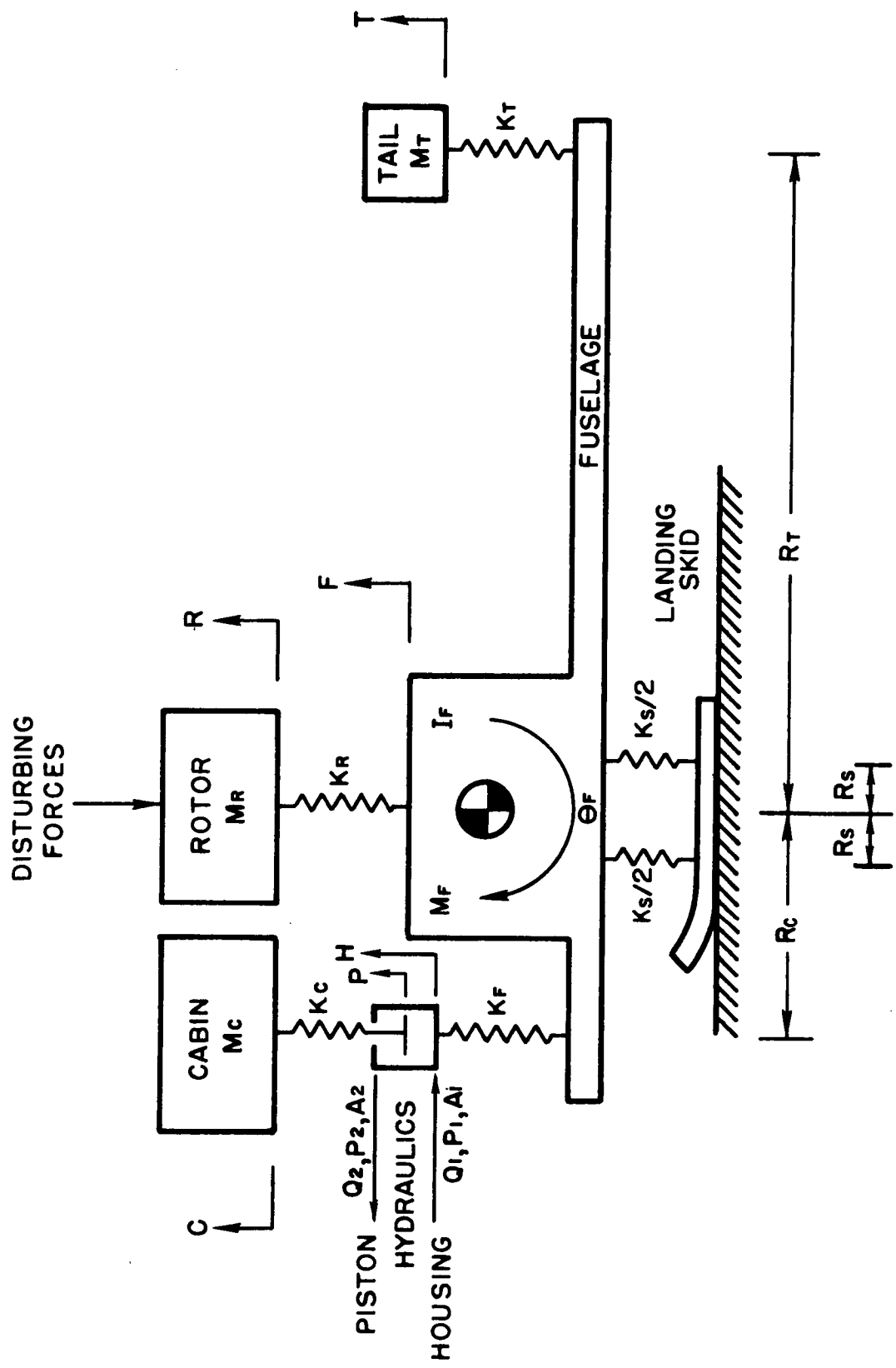
Figure 13: Four-Mass Model of XH-51 Helicopter
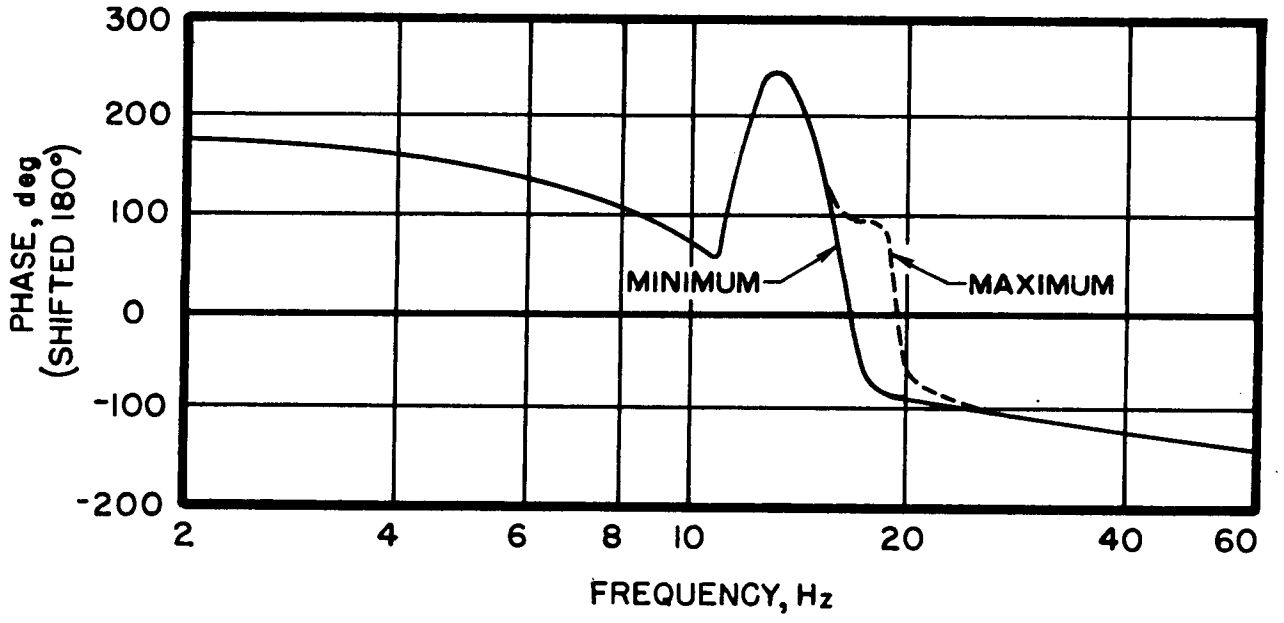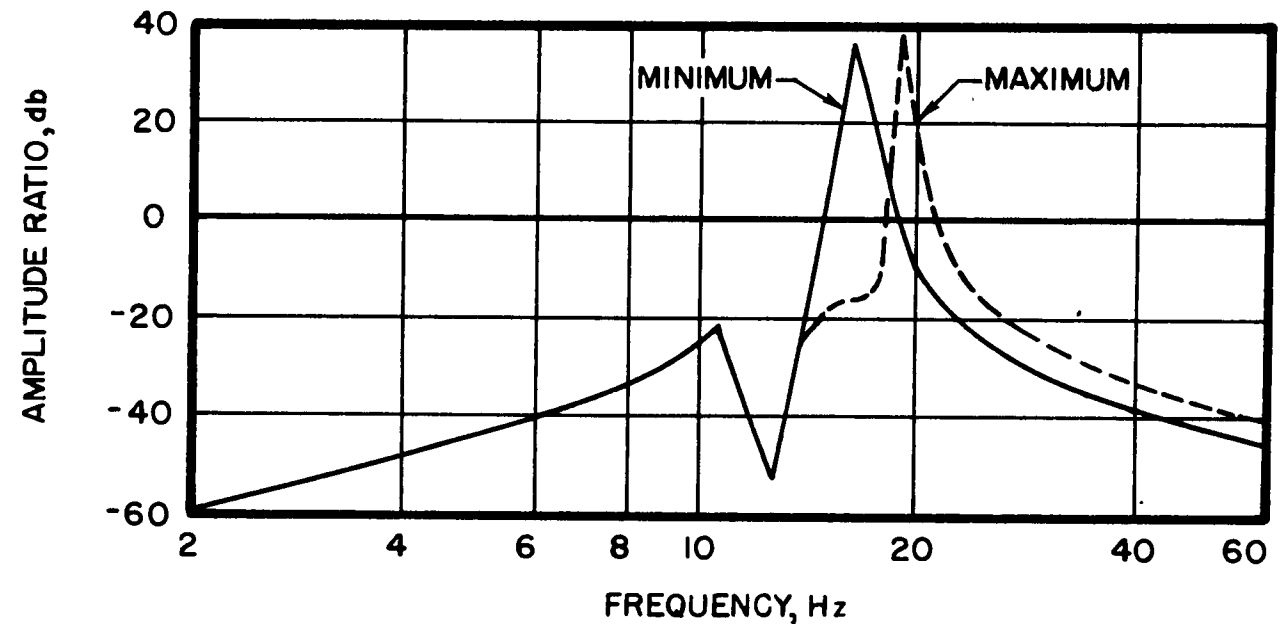
Figure 14: Open Loop Transfer Function of XH-51 Helicopter
Four-Mass Model with 18 Hz Notch Control Function
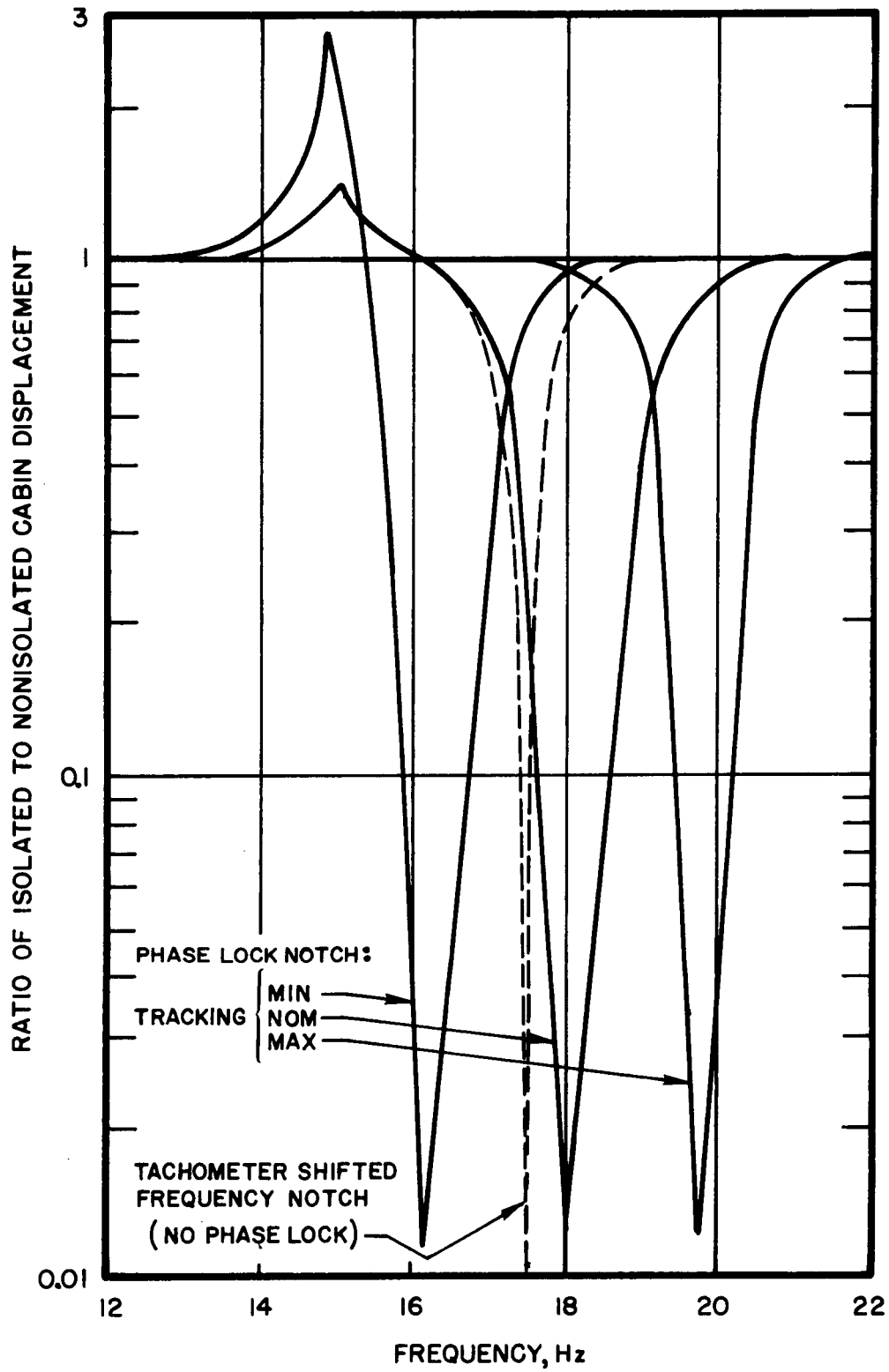
Figure 15: Calculated Active Cabin Isolator Effective Transmissibility
With Phase Locked Tracking Notch
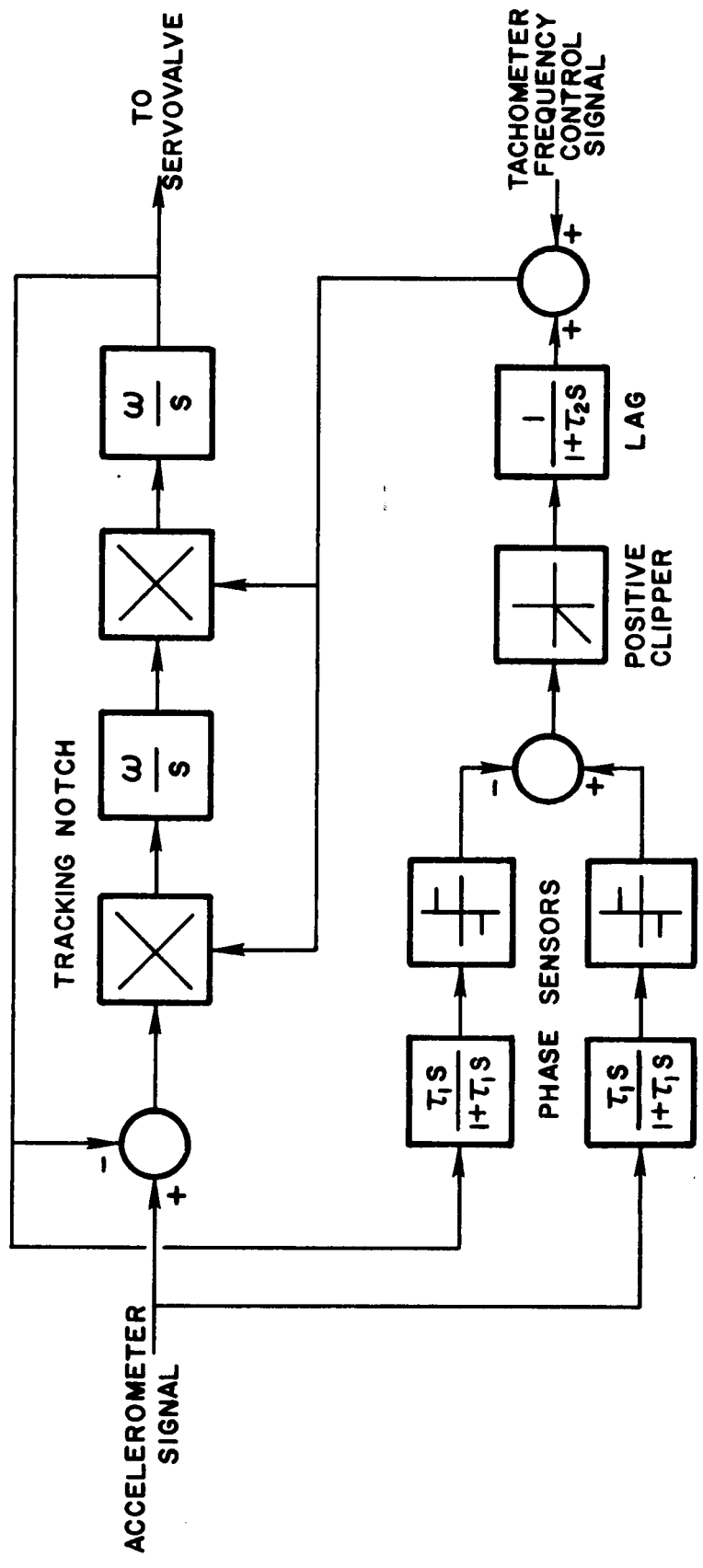
Figure 16: Block Diagram of Notch Function
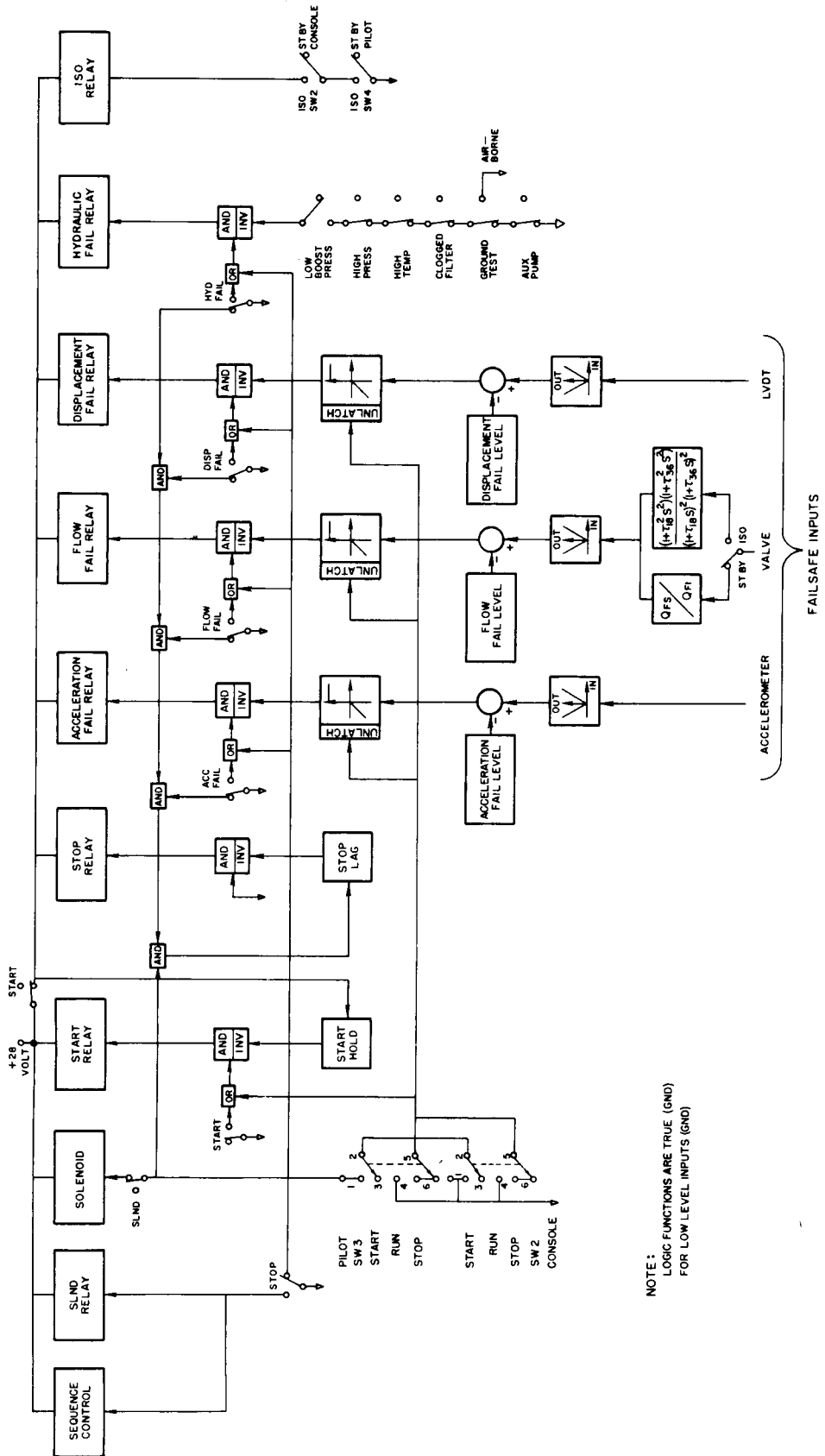
Figure 17: Failure Logic Block Diagram of XH-51 Active Isolation System
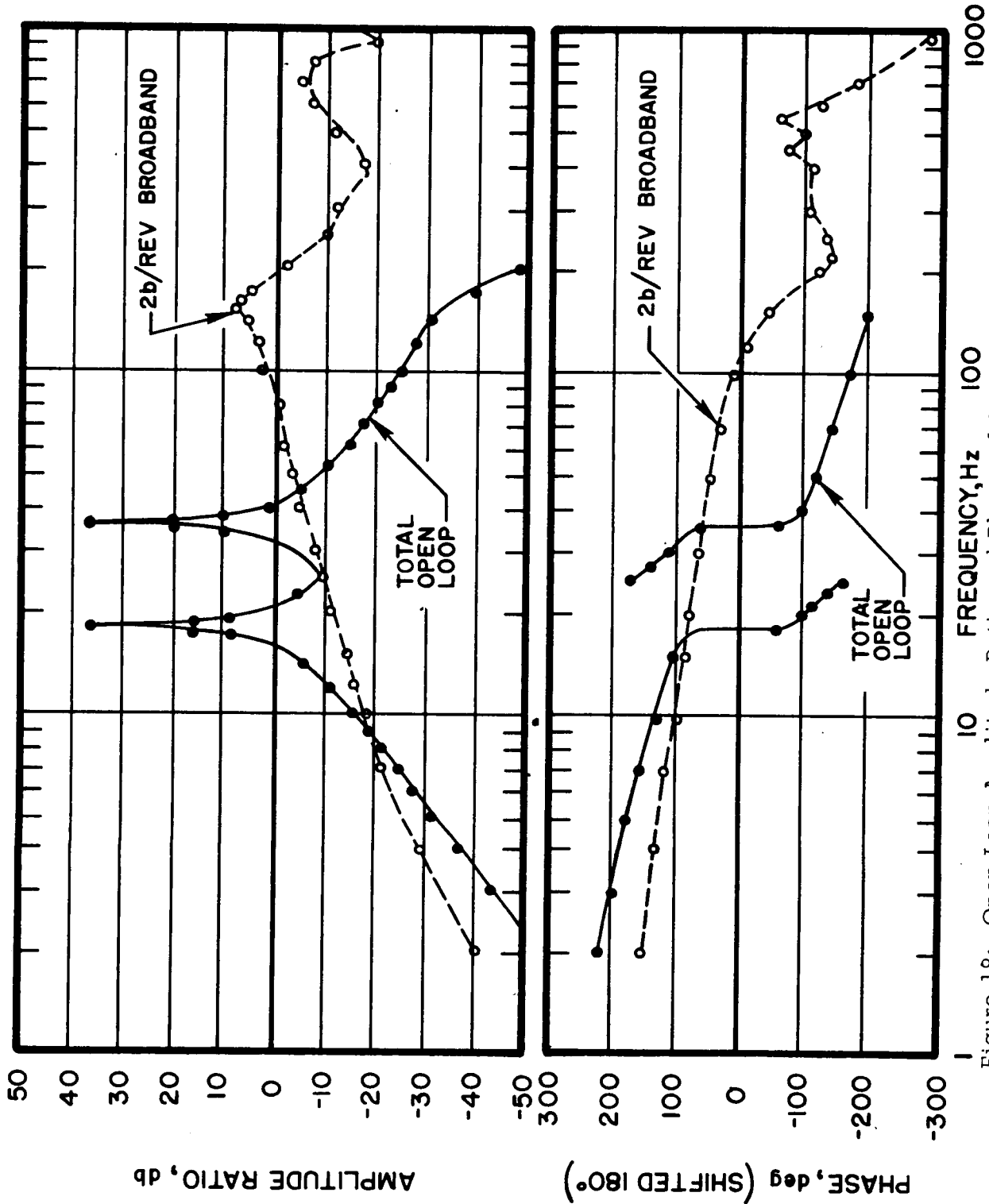
Figure 18: Open Loop Amplitude Ratio and Phase of Active Seat Isolator Vertical Transfer Function Measured During Laboratory Tests
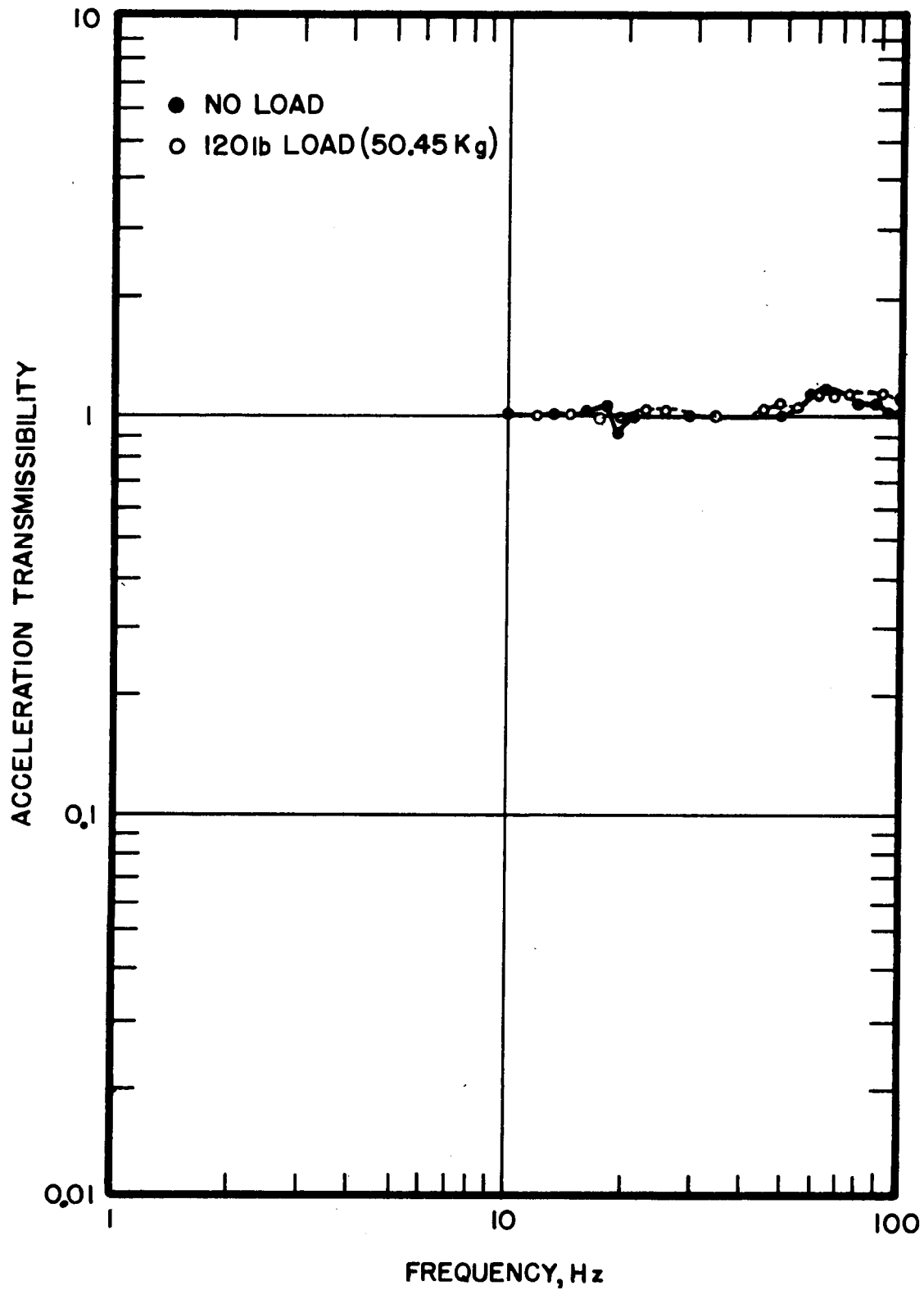
Figure 19: Vertical Transmissibility of Active Seat Isolator in
Locked-Out Mode Measured During Laboratory Tests
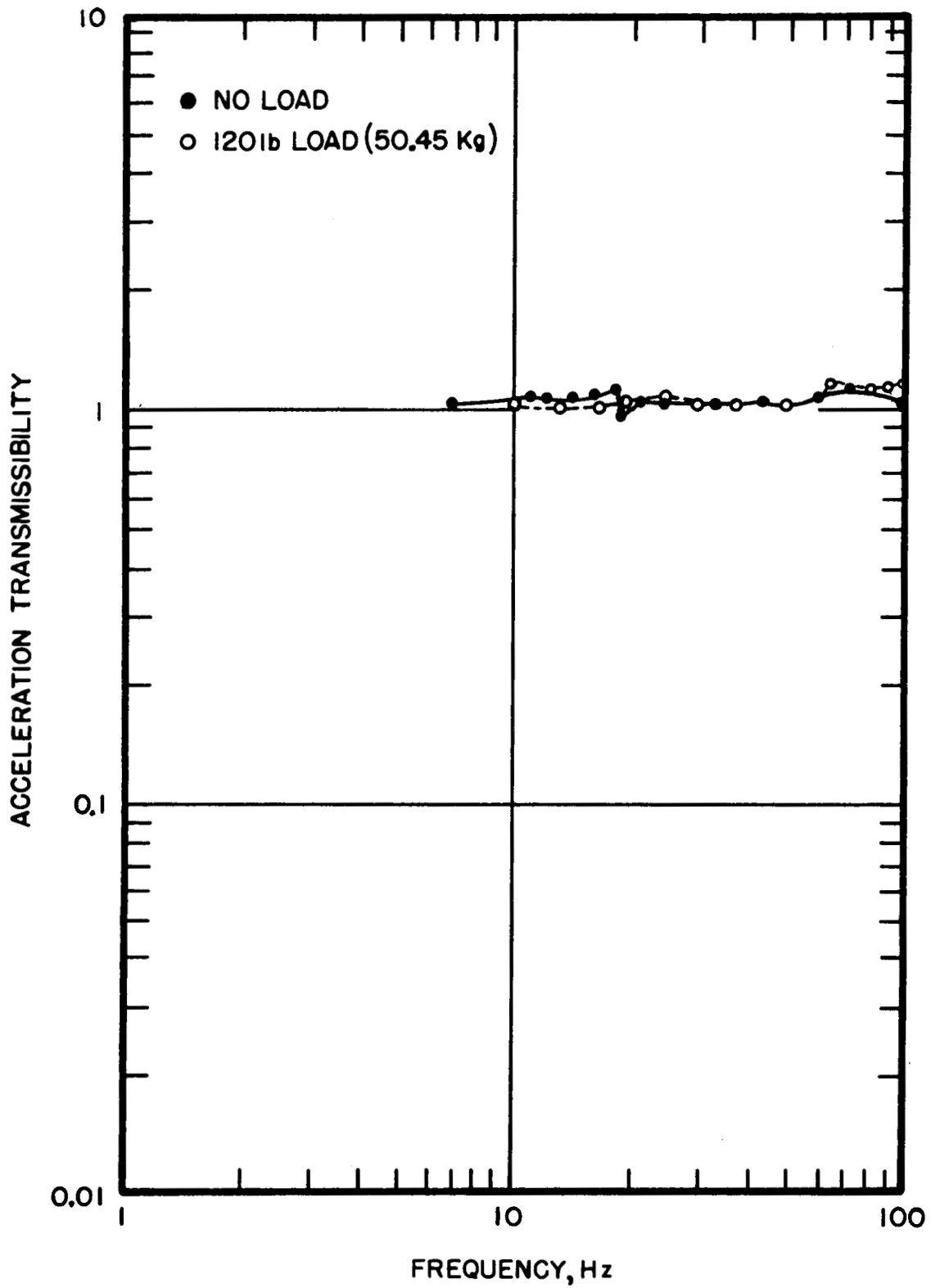
Figure 20: Vertical Transmissibility of Active Seat Isolator in
Standby Mode Measured During Laboratory Tests
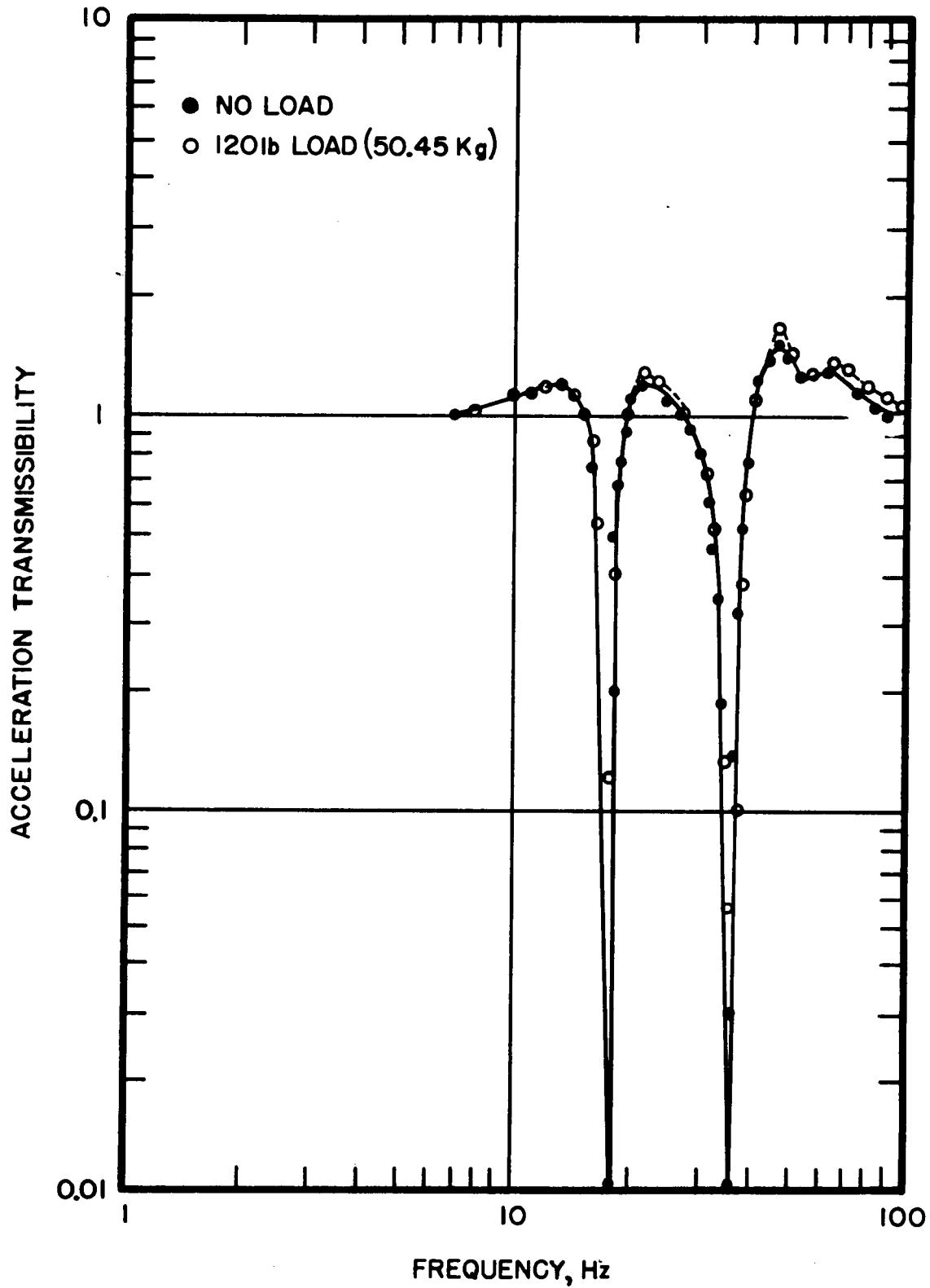
Figure 21: Vertical Transmissibility of Active Seat Isolator in
Isolate Mode Measured During Laboratory Tests
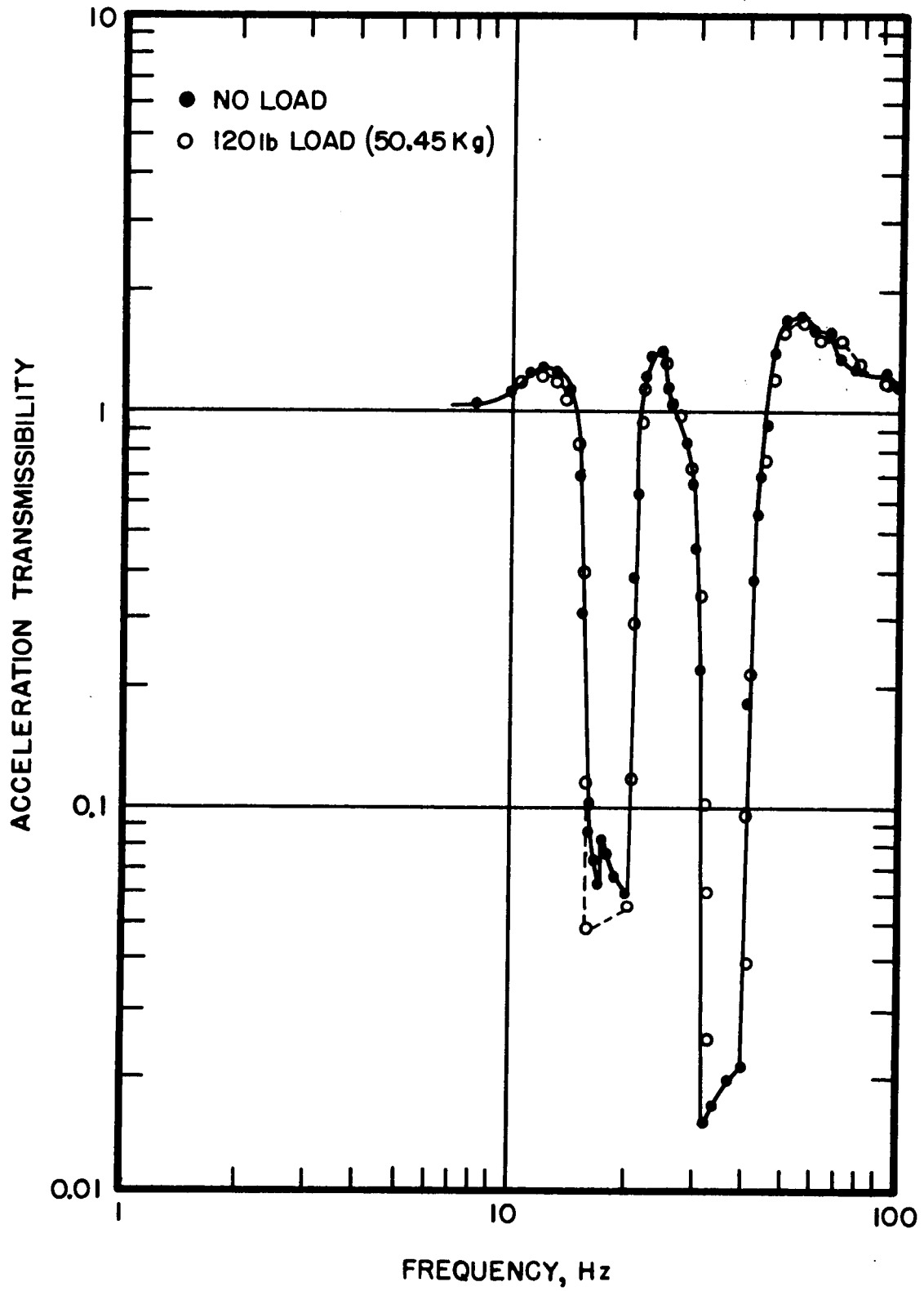
Figure 22: Vertical Transmissibility of Active Seat Isolator in Isolate
Mode With Tracking Measured During Laboratory Tests
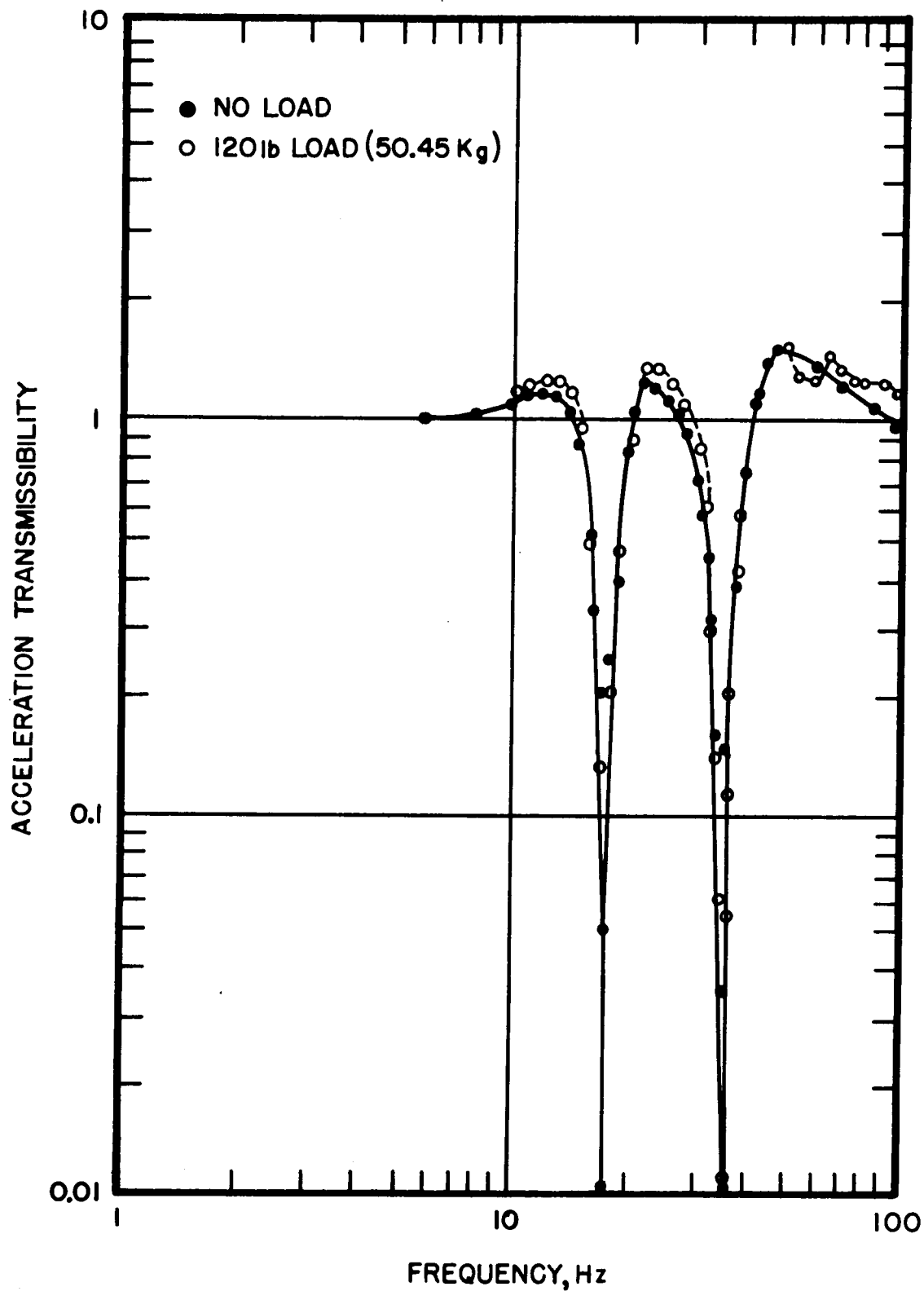
Figure 23: Vertical Transmissibility of Active Seat Isolator in Isolate Mode
With Phase-Lock Notches Measured During Laboratory Tests
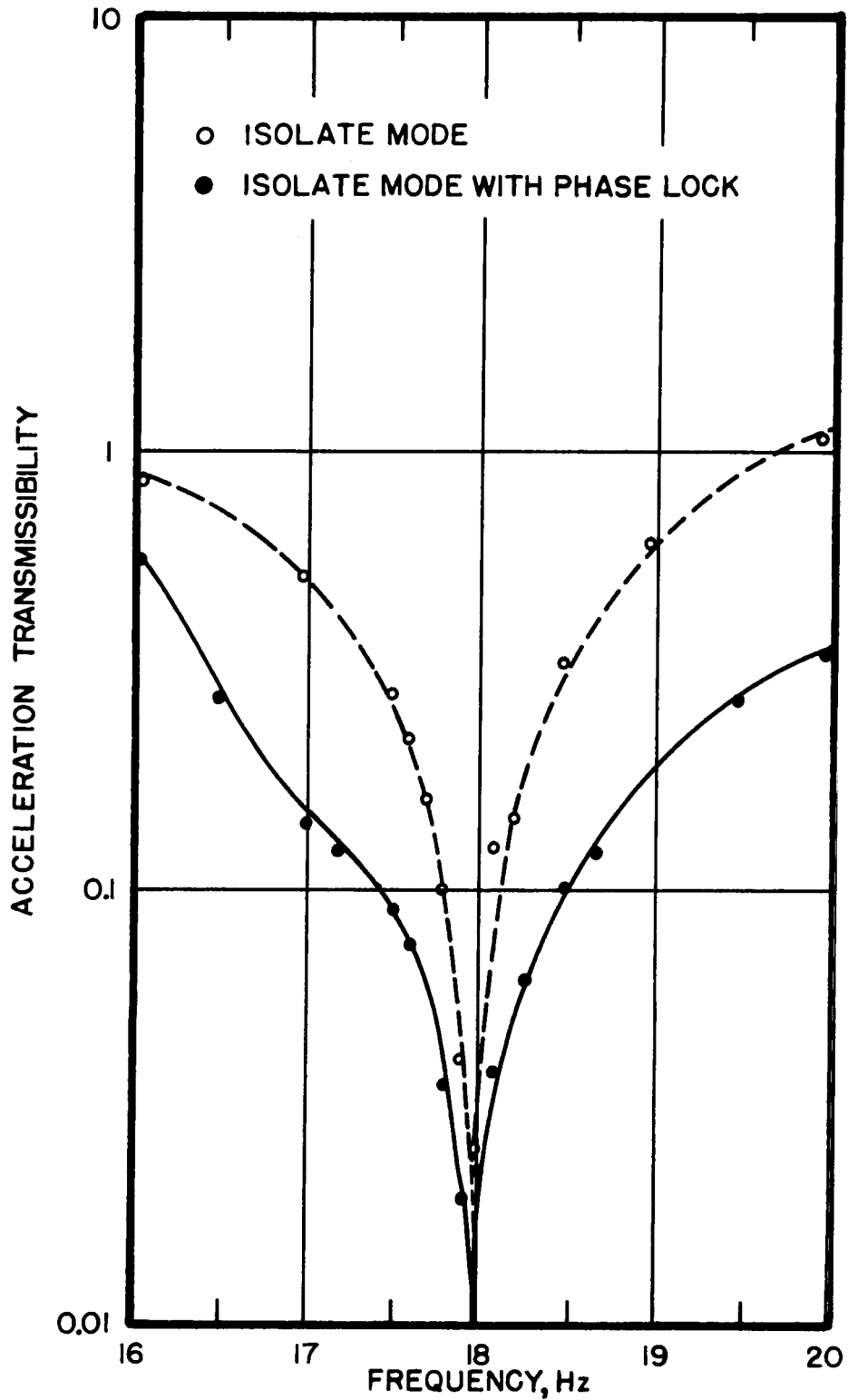
Figure 24: Comparison of Vertical Transmissibility of Seat Actuator In the Neighborhood of b/rev With and Without Phase-Lock Notches Measured During Laboratory Tests
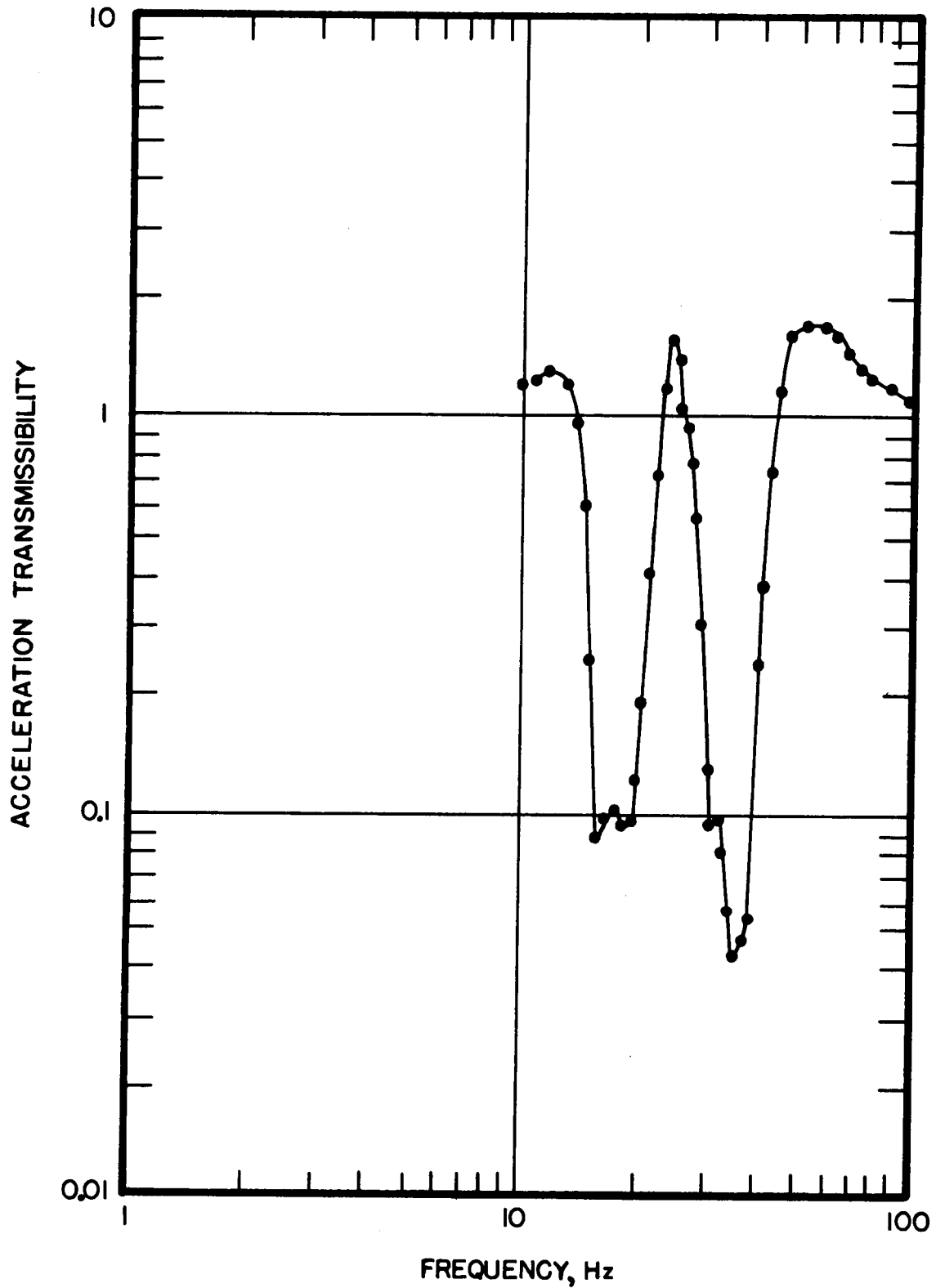
Figure 25: Vertical Transmissibility of Seat Actuator in
Isolate Mode With Tracking and Phase-Lock
Notches Measured During Laboratory Tests
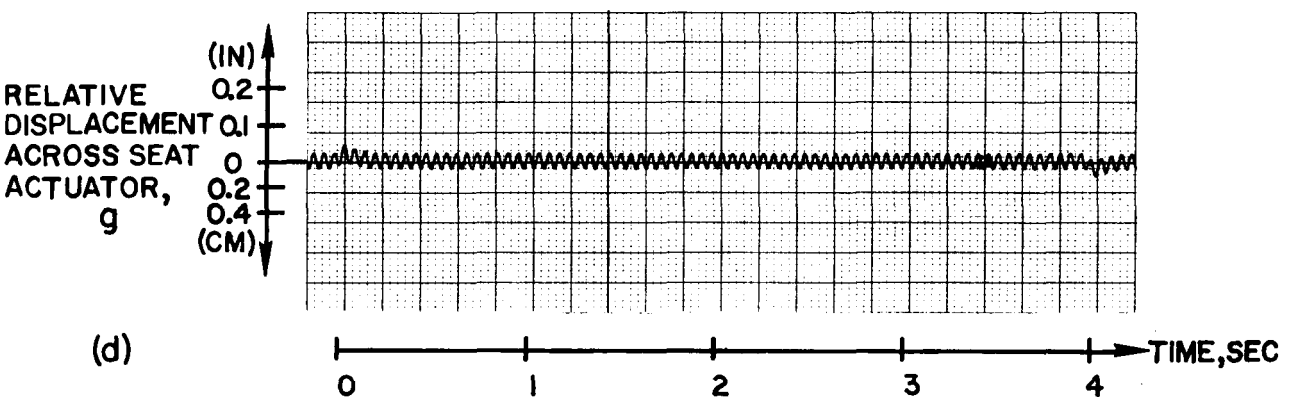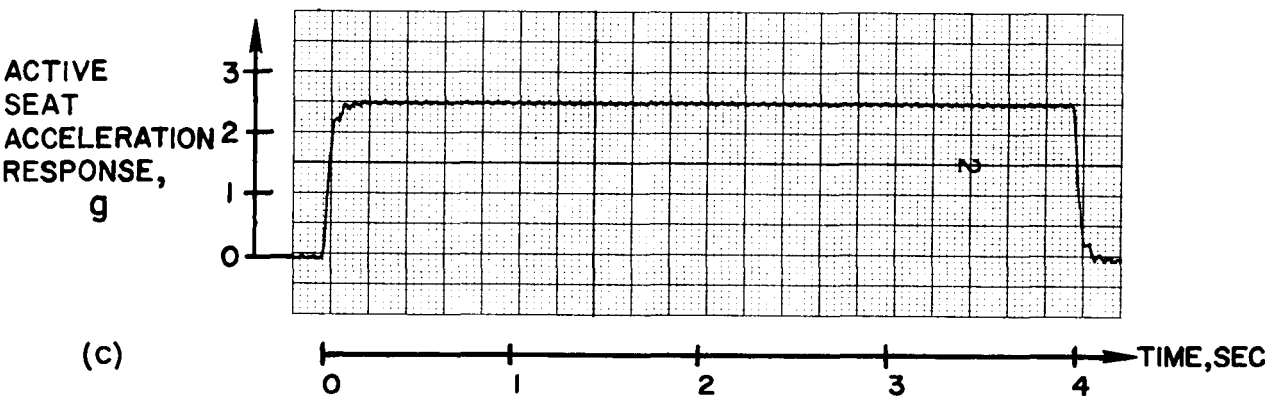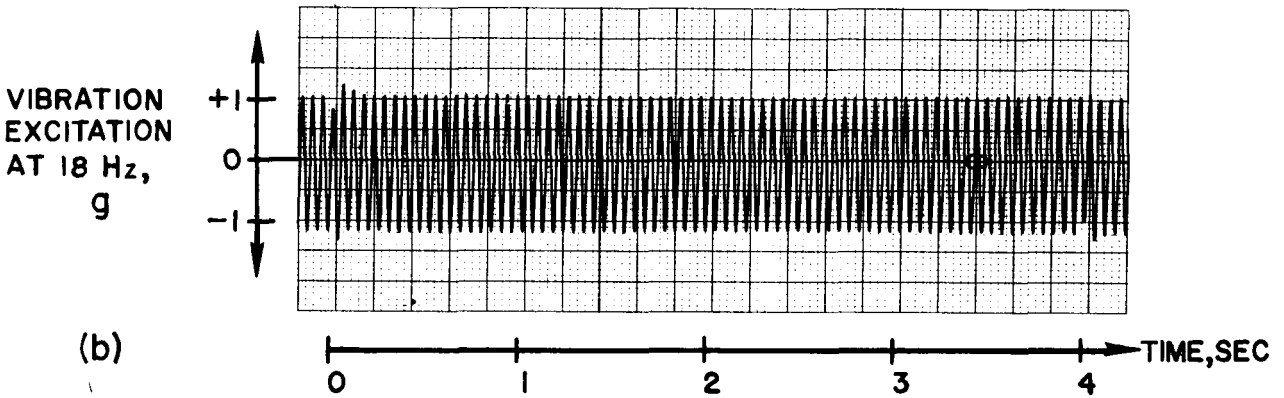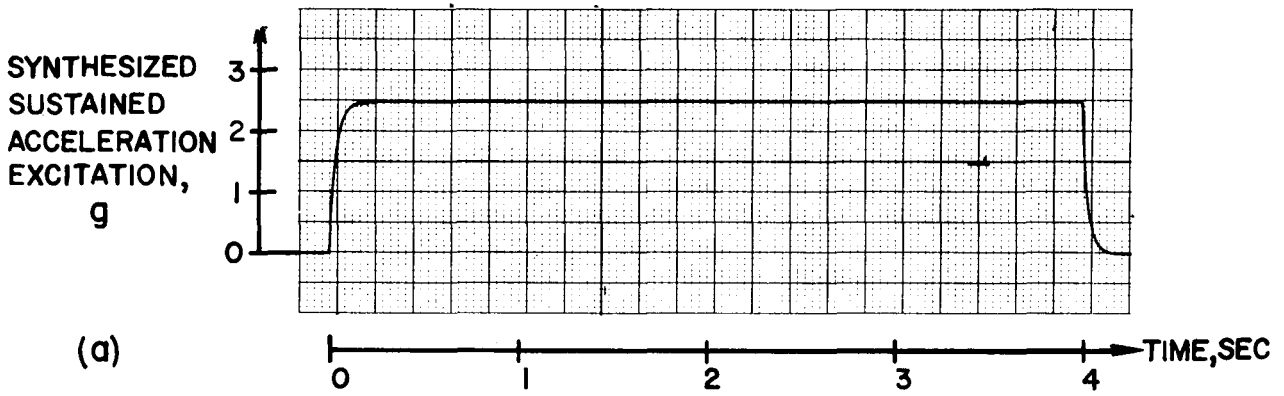
Figure 26: Response of Active Seat Actuator to Combined
Vertical Sustained Acceleration and Vibration
Excitations Measured During Laboratory Tests
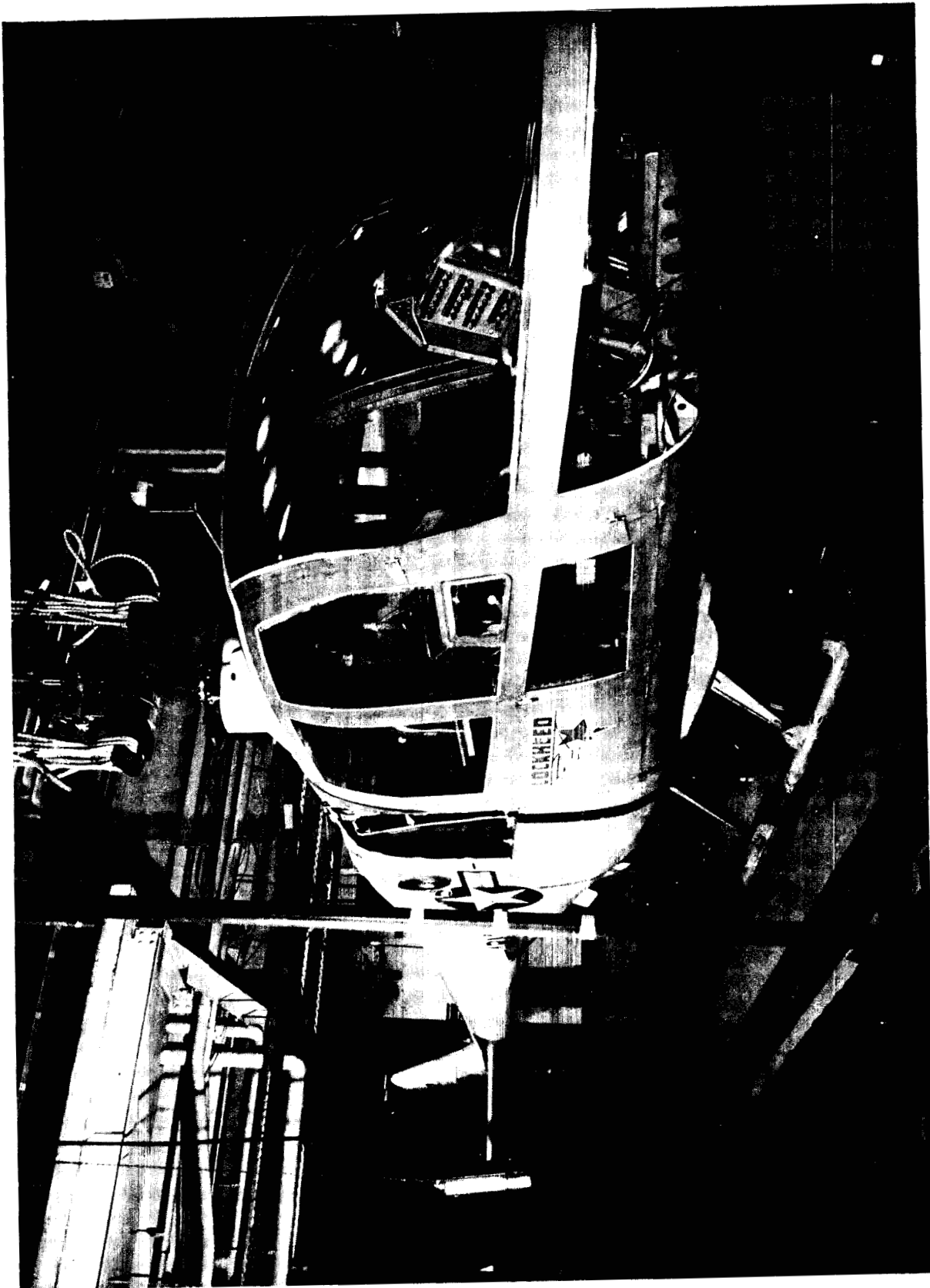
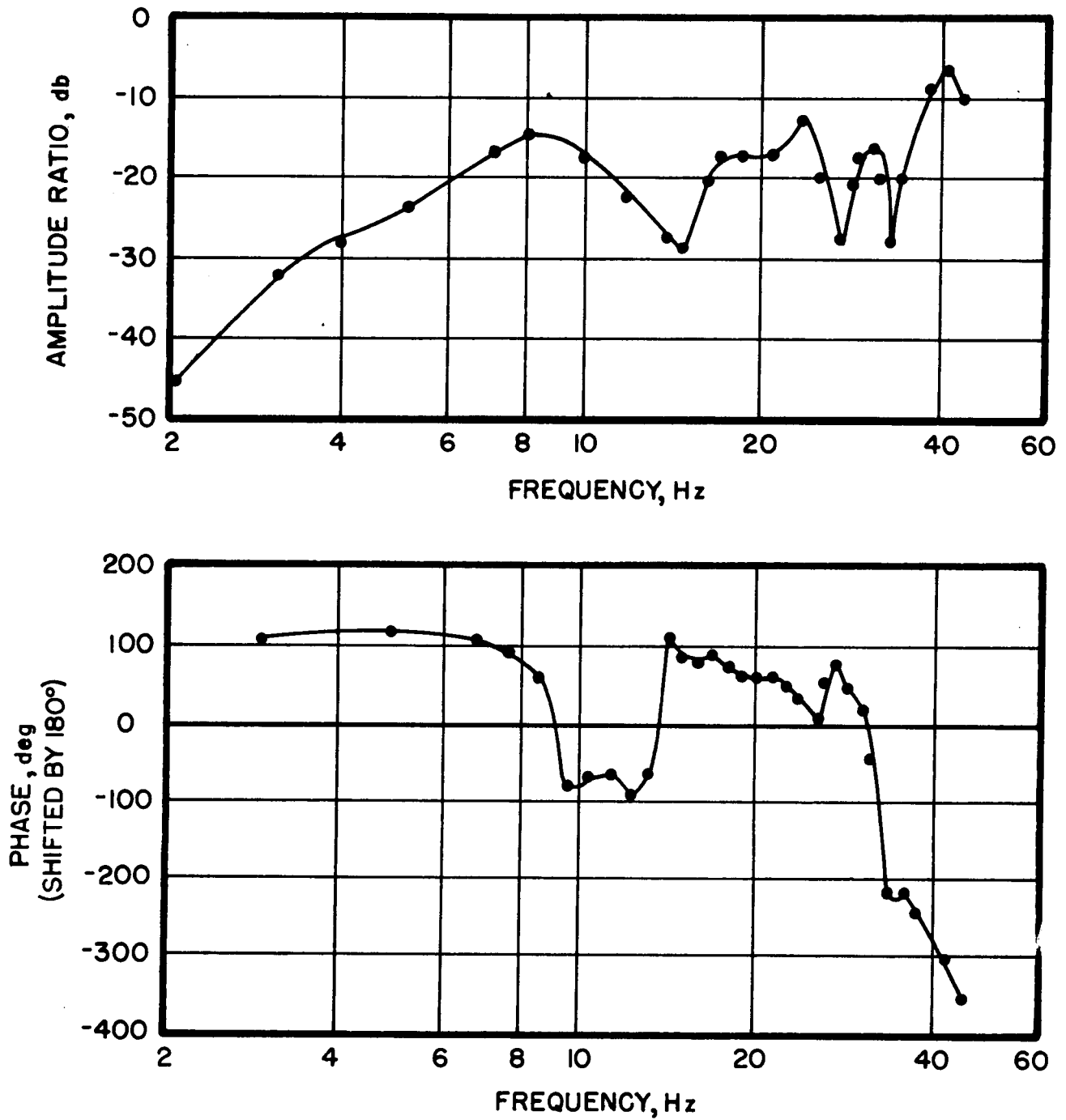Figure 27: Installation of XH-51A Fuselage For Ground Vibration Testing

Figure 28: Broad-Band Open Loop Transfer Function of Active Cabin
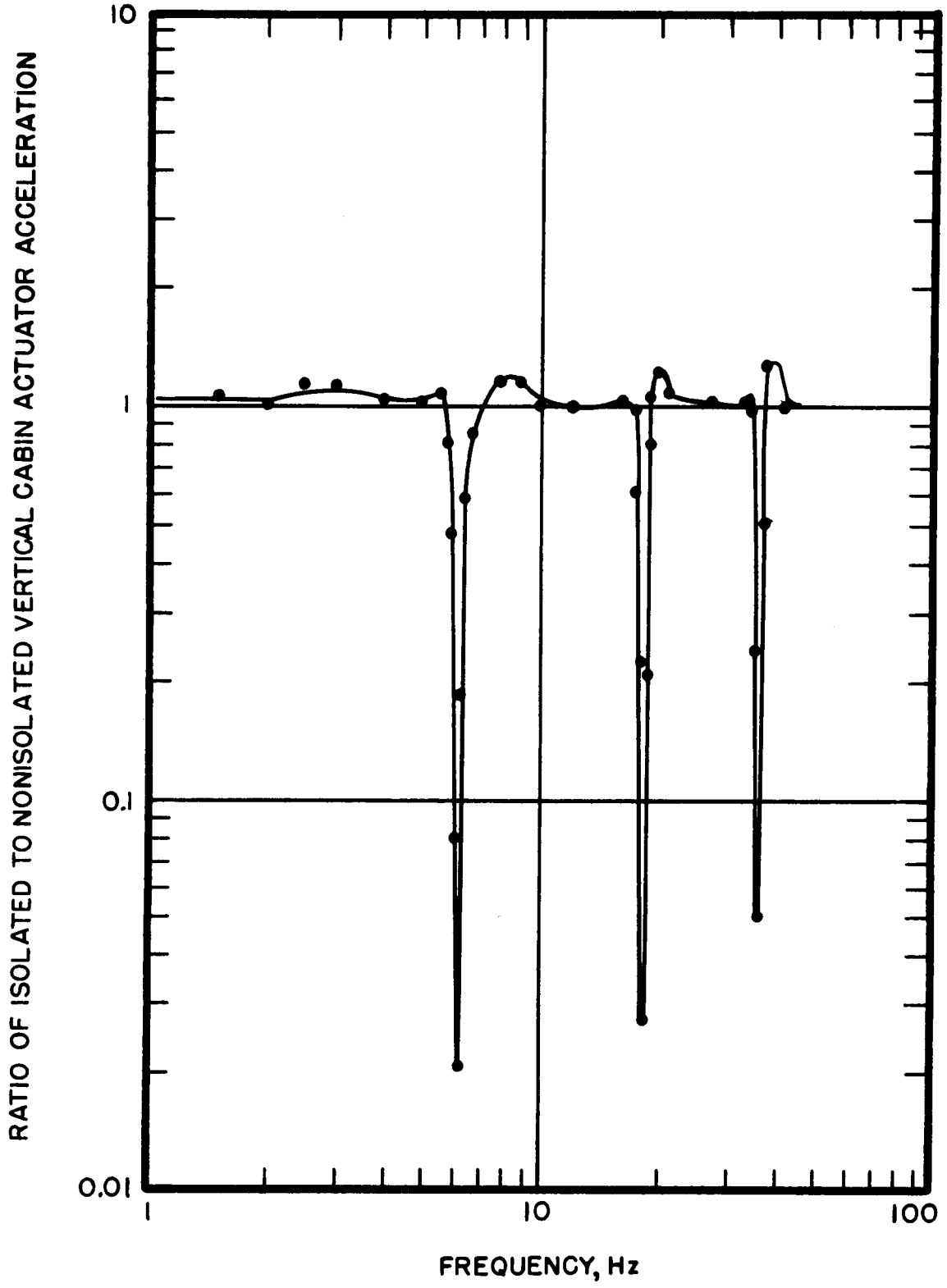Isolator at b/rev Measured During Ground Testing

Figure 29: Vertical Effective Transmissibility of Cabin
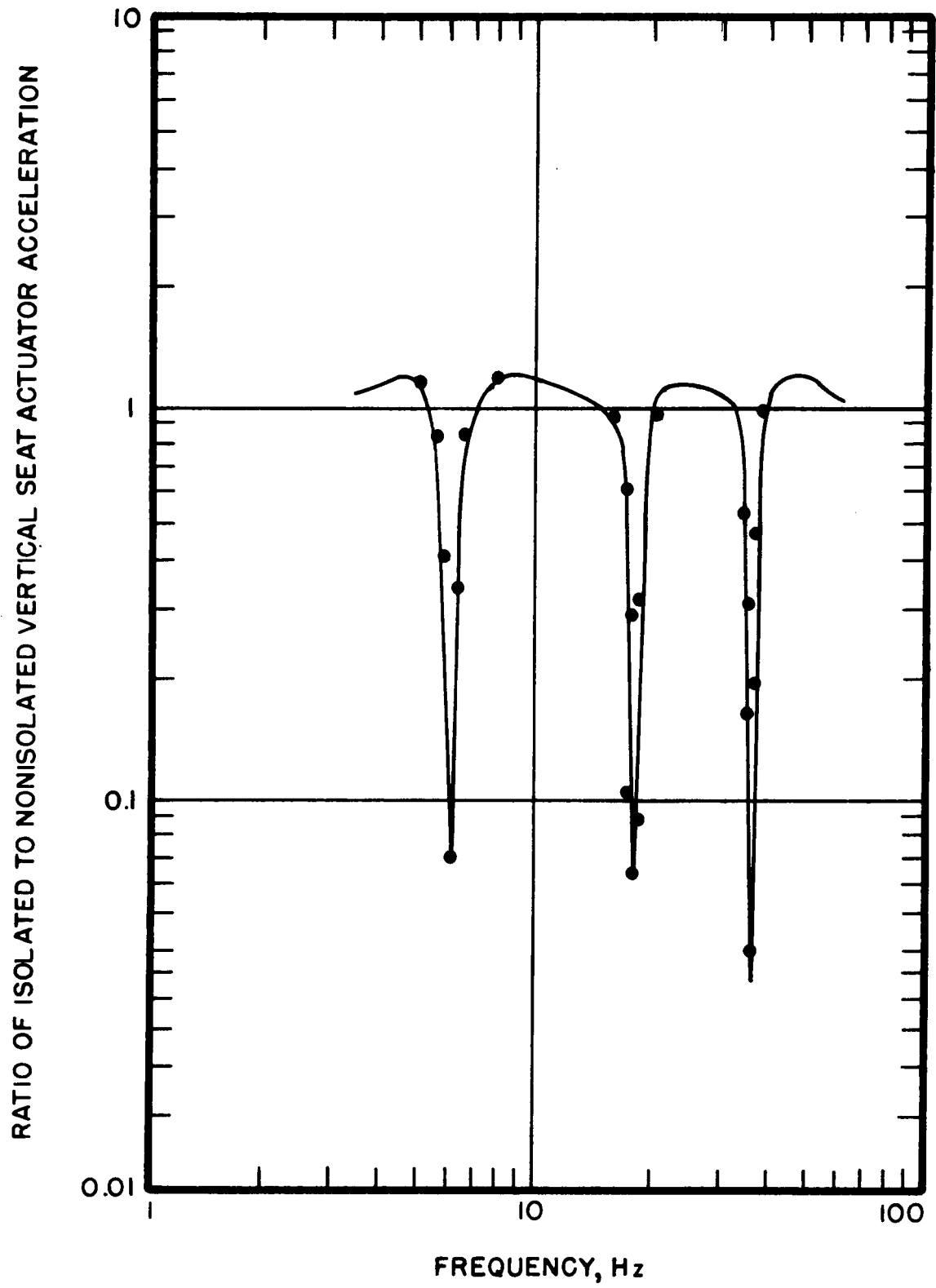Isolator Measured During Ground Testing

Figure 30: Vertical Effective Transmissibility of Seat
Isolator Measured During Ground Testing